UNIVERSITY OF TARTU

Faculty of Science and Technology

Institute of Technology

Harti Kiveste

FLUID LENS DEVICE
CONSTRUCTION AND ACTUATOR PERFORMANCE BASED ON ELECTROACTIVE POLYMERS

Master Thesis

Supervisor: Prof. Rudolf Kiefer

Tartu 2013

Table of contents

INTRODUCTION

Autofocus fluid lens device, for example by Varioptics, based on water/oil interfaces forming a spherical lens by the meniscus of the liquid that can be switched by applying high voltage to change from convex to concave divergent lens. In this work the main goals are the construction an autofocus fluid lens device to investigate membrane actuators based on actuator material such as conductive polymers and ionic polymer metal composites (IPMC). We applied between electrolyte/oil interfaces a membrane actuator with in the middle formed hole to obtain a meniscus between both liquids. At applied voltage the actuator can change the meniscus from concave to convex shapes. To investigate membrane actuation displacement we applied conductive polymers such as PPy doped with TFSI and PPy doped with DBS at different polymerization conditions (temperature, time and solvent) to evaluate which conductive polymer shows the best membrane actuation. Membranes with conductive polymer actuators are less described in literature due their low degree of freedom and therefore low displacement properties. To improve the membrane actuation properties we changed the membrane design by cutting it at different shapes and elaborated in simulation and real measurements the optimum displacement. We applied a new design of the membrane and could observe small lens changing properties. The relative low voltage (< 1.0 V) of the EAP membrane actuator make the autofocus fluid lens applicable in portable electronics such as cell phones, laptop and tablet computers.

1. OVERVIEW

1.1. Autofocus fluid lens

Autofocus fluid lens can be divided into two primary types such as transmissive and reflective. The reflective type works as variable mirror applied in reflector telescopes. The principle of the reflective liquid lens is based on variable mirror, for example by using mercury applying centripetal forces to create a smooth reflective concavity, that reduces the cost ten times of such lenses, compared to traditional way fixed on curved glass. The biggest telescope based on liquid reflective mirror (mercury) is placed at University of British Columbia.

In contrast to the reflective fluid lens, the transmissive fluid lens based on active change of the convex concave lens shape over immiscible fluids with different refractive index. The change of the liquids can be obtained mechanically or electrically. The advantages of such transmissive fluid lenses are the high optical quality in the range of 10µm. The principal working mechanism is demonstrated in Figure 1.

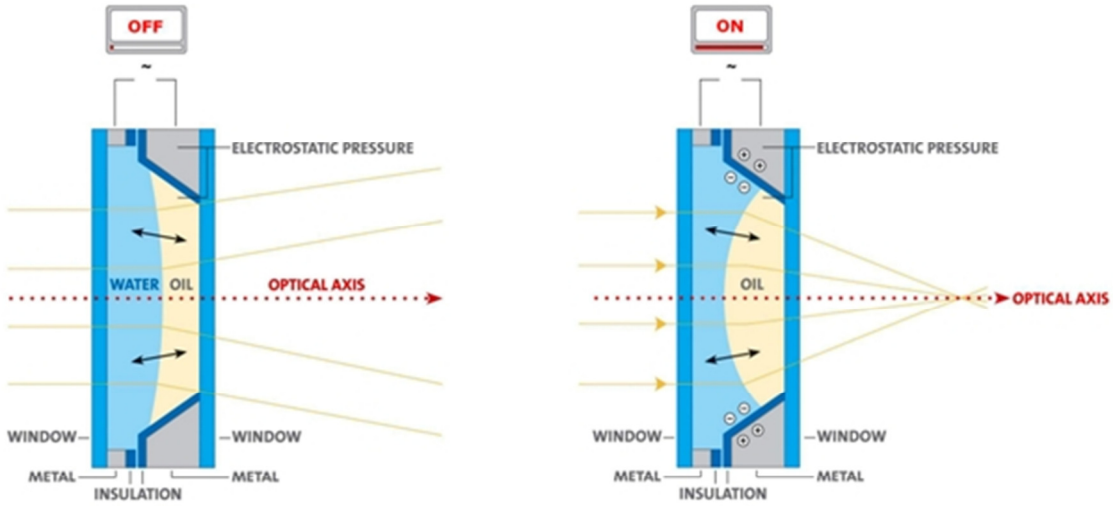

Figure 1. Design of the Varioptic fluid lens[1]

The liquid lens uses two isodensity liquids, an insulator and a conductor. The variation of voltage leads to a change of curvature of the liquid-liquid interface, which in turn leads to a change of the focal length of the lens[2]. A similar design of the liquid lens cell has been made by Phillips using electrowetting techniques. The difference can be found in the coating of the tube with one part hydrophobic and the other with hydrophilic material forming a hemispherical lens shaped mass at

the end of the tube [3]. Both electrical induced shape lenses devices need high voltage between 2-4 kV to obtain focus changes. The mechanical manipulation of the surface tension between the two liquids are introduced over functional elements such as pumping liquids forcing the lens shape to change based on the Singapore type (Figure 2) [3].

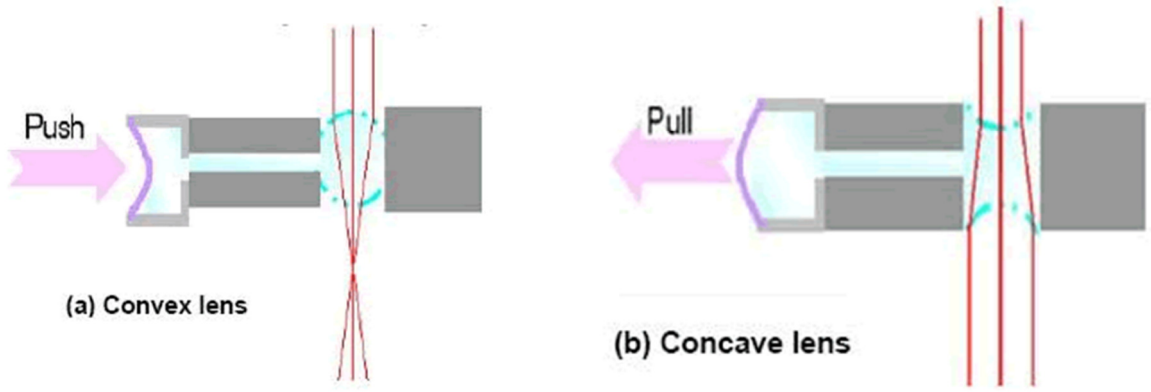

Figure 2 Singapore type of autofocus liquid lens cell based on two chambers with pumping solution and lens shaping membrane

Extremely small cameras and many cell phones simply don't have enough room for a rigid lens. An adaptive liquid lens, however, enables small cameras to focus without needing any extra room. But traditional approaches, which use an electric current to change the surface shape of a liquid, require a lot of power.

1.2. 2-Liquid fluid lens with membrane actuator

When we take two insoluble liquids like oil and aqueous electrolyte and separate those with a membrane actuator, which has a hole inside, then the two liquids, will form a meniscus (Figure 3). By moving the actuator membrane it is possible to control the shape of the meniscus. If we guide light through the hole inside the membrane, the meniscus will work as a lens. By altering the potential applied to the membrane actuator it's possible to seamlessly control the focal length of the lens.

In order to control the change of the shape of the lens mechanically with an EAP actuator, different studies have been carried out. Simulations revealed, 100 –200µm displacement of membrane edge is necessary for constructing a useful lens[4].

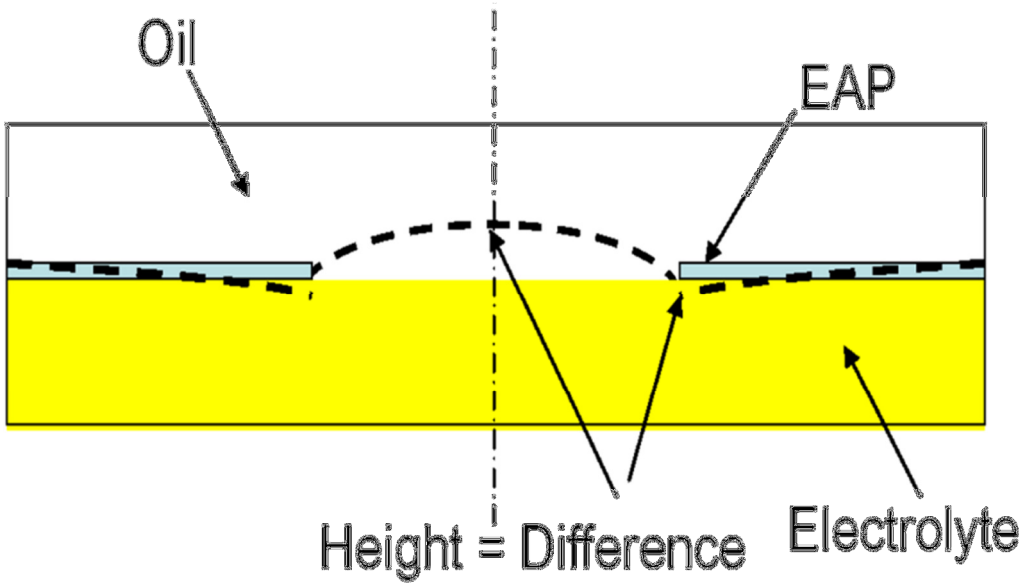

Figure 3 Principle of 2-liquid membrane actuator forming a meniscus between two fluids applicable for lens changes[4]

1.3. Electroactive polymers (EAP)

EAP can be divided into two major categories based on their activation mechanism including ionic and electronic (Table 1). Coulomb forces drive the electronic EAP, which include electrostrictive, electrostatic, piezoelectric and ferroelectric. This type of EAP materials can be made to hold the induced displacement while activated under a DC voltage. These EAP materials have a greater mechanical energy density and they can be operated in air with no major constraints. However, the electronic EAP require high activation fields (>100 V/μm) that may be close to the dielectric breakdown level. In contrast to the electronic EAP, ionic EAPs are materials that involve mobility or diffusion of ions and they consist of two electrodes and an electrolyte. The activation of the ionic EAP can be made by as low as 1-2 volts and mostly a bending displacement is induced. Examples of ionic EAP include gels, polymer-metal composites, conductive polymers, and carbon nanotubes (CNT). They need to maintain wetness and they pose difficulties to sustain constant displacement under activation of a DC voltage (except for conductive polymers).

Table 1: List of different EAP types

Electronic EAP	Ionic EAP
Electrostrictive Graft Elastomers	Conductive Polymers (CP)
Electrostrictive Paper	Ionic Polymer Metallic Composite (IPMC)
Electro-Viscoelastic Elastomers	Carbide-derived Carbon (CDC)
Ferroelectric Polymers	Carbon Nanotubes (CNT)
Liquid Crystal Elastomers (LCE)	Ionic Polymer Gels (IPG)
	ElectroRheological Fluids (ERF)

The induced displacement of both the electronic and ionic EAP can be designed geometrically to bend, stretch or contract. However, bending actuators have relatively limited applications due to the low force or torque that can be induced. EAP materials are still custom made mostly by researchers and they are not available commercially.

1.3.1. EAP actuators for Auto-Focusing Fluid Lens device

For constructing a membrane actuator for fluid lens applications in cell phones it is necessary to operate with low energy supply, position control and reliability. Under DC voltage the bending position has to be maintained to obtain the desired focal length of the liquid lens. To obtain membrane actuators with enough displacement the choice of thickness, stiffness and size of the membrane need to be considered. The actuator material based on EAP needs to fulfil certain requirements to be suitable in autofocus fluid lens applications:

- The actuation force needs to be high enough to overcome the surface tension between oil/electrolyte
- The displacement of the membrane actuator in the minimum must be 200 µm to change the formed meniscus between oil and aqueous electrolyte[4]
- The membrane actuation should be driven under 1 V
- The actuation speed should be in the range of 0.1-10 Hz
- The actuator membrane should show no creep
- The long term cycling of the actuator membrane should exceed more than 100.000 cycles

Two different types of ionic EAP based on CP and IPMC are investigated in this work to evaluate which gives under certain conditions the membrane actuation to change the meniscus between oil and aqueous solution.

1.3.2. Conductive polymers (CP)

Conductive polymers such as Polypyrrole (PPy) and Poly-3, 4-ethylenedioxythiophene (PEDOT) are the most applicable materials in the preparation of CP actuators[5]. Many applications can be found where the electronic properties of this material are used in form of light emitting diodes [6], batteries [7], electrochromic devices [8], sensors [9], and biomedical applications [10]. The choice of conductive polymer material in actuator functionality requires a specific procedure in actuator material such as flexible non-conductive membranes, conductive coatings and electrochemical polymerization.

From the theoretical point of view the radical polymerization of monomer units over cascade different steps leads to insoluble conductive polymer chains (12-16 monomer units) which forms a polymer network[11, 11] . Several parameters (electrolyte and monomer concentration, temperature, electrolyte, solvent, electrochemical polymerization condition, thickness of CP layer [12 13 14]) can be changed to obtain conductive polymer networks with different actuator properties. Polymerization can achieved with different electrochemical methods, whereby the goal is to obtain a dense conductive polymer film on the working electrode. Galvanostatic (constant current) methods provide dense conductive polymer films, whereby the potential, which is important for the oxidation level of the conductive polymer, cannot be controlled. Potantiodynamic polymerization has a constant scan rate comparable to running a cyclic voltammogramm. Potentiostatic methods provide a constant potential and in general, the effects at different polymerization potentials in CP actuator materials are recently studied [15 1617].

The working electrode can be a non conductive polymer such as PVDF, PET or other plastic coated with a thin conductive layer that was in traditional studies an inert metal such as sputtered platinum or vaporized gold. If the metal phase changes to other conductive coating material, such as a chemically coated CP [18] material, it needs to be considered that the resistivity of such material is low enough (< 1 MΩ) to obtain electrochemical CP deposition.

The basis for conductive polymer actuation is considered to largely involve swelling of the polymer from ion and solvent ingress during oxidation and reduction cycles, achieved at low operating voltages. To balance the charge neutrality, ions from surrounding electrolyte either enter or exit the conductive polymer inducing a swelling or contraction of the material.

1.3.3. IPMC actuators

Ionic polymer-metal composites are representative to the group of ionic EAP and are, in their actuation mechanism, different from conductive polymers. The principal assembly is based on perfluorinated polymer membrane coated with inert metals such as platinum on both sides[19]. In most cases the choice of perflourinated polymer membranes falls on Nafion polymers where a fixed negative charge makes the counterions (cations) movable between both metallic layers. Two explanations are given to explain the actuation of IPMC, as a consequence of solvent (water) molecule migration dragged by mobile ions or due to the charge unbalance of the polymer backbone[20]. The main disadvantage of IPMC actuators in comparison with the conductive polymers is the back relaxation phenomenon under DC voltage[21]. The advantages and disadvantages for IPMC and CP actuators are presented in Table 3.

Table 2: Advantages/Disadvantages of IPMC and CP actuators

Actuator type	Principle	Advantage	Disadvantage	Types
IPMC	Electrostatic forces and mobile cations causes actuation	Low voltage , 1-5V High bending displacement f = 1 – 25 Hz	Sensitive to dehydration Back relaxation under DC	Polymer: Nafion® Flemion® Cations: TBA^+, Li^+ Metal: Pt, Au
Conductive polymers	Reversible volume change at redox cycles inflected by ions and solvent	Low voltage, < 1V High bending displacement Frequency 1-100 Hz	Low bending force Need electrolyte	PPy, PEDOT, PANi, PPh

2. MATERIAL AND METHODS

2.1. EAP membrane actuators used for measurements

All conductive polymers we applied for testing were polymerized on 100µm PVDF membrane. The first one was PVDF gold coated membrane all others were chemically coated with PPy. For chemical coatings we applied PVDF membranes, covered them in pyrrole and immersed in aqueous solution with oxidant (0.075 M ammoium persulfat, 60^{o}C). The first membrane immersion time was set for 30s, second 45s and third 60s (Figure 5). This method was developed by Rauno Temmer et al.[19].

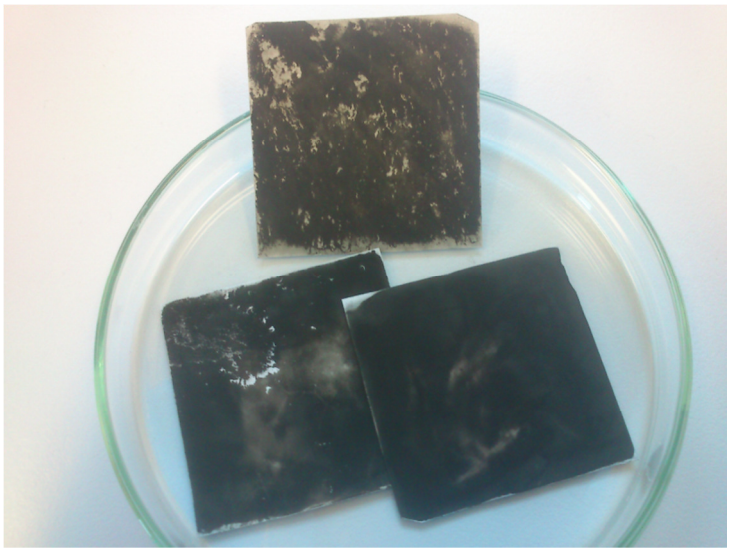

Figure 4. Chemically polymerized PVDF membranes with PPy (both sides)

For electrochemical polymerization we applied galvanostatic polymerization technique with current density of 0.1mA/cm^2. We applied three different polymerization conditions which differ by electrolyte, solvent, polymerization time and temperature. The conductive polymer polypyrrole (PPy) doped with TFSI$^-$ (bis(trifluoromethane)sufonimide) was electrochemically polymerized in a two electrode cell (counter electrode and reference electrode: stainless steel sheet, working electrode: conductive PVDF membrane) in propylene carbonate (1.0M LiTFSI, 1.0M pyrrole) at -33^{0}C. The membrane type coated with gold and deposited with PPyTFSI (20 µm thickness) we named membrane A1, those coated with chemical PPy we named membrane A2. The polymerization in aqueous electrolyte (0.2 M pyrrole, 0.2 M NaDBS (sodium dodecyl benzensulfonate), water:ethyleneglycole 1:1) took place in same electrode arrangement. At polymerization time of 11.11h at -33^{0}C we obtained membrane B1 (PPyDBS, 20µm thickness)

and at polymerization time of 1.11h at -5^0C we obtained membrane B2 (PPyDBS, 2μm thickness). In all cases the membrane was polymerized at given thickness each side of the conductive PVDF membrane in trilayer design. The membranes were cleaned of the polymerization electrolyte and soaked for at least 12h in the electrolyte that was used for actuation. Polymerization curves for all membranes can be found in **Error! Reference source not found.**.

3. FLUID LENS MEASUREMENT DEVICE

3.1.1. Designing the device

For testing the liquid lens with an EAP, we built a device suitable to determine the membrane actuator displacement and lens changes. We started with a device that is able to measure different size of membrane actuator by simple adjustments. Requirements for the device were following:

- easy to open and close
- easy to fill with electrolyte
- must mount 2 electrodes: working electrode and counter electrode
- distance to the counter electrode should be changeable
- it must be possible to make experiments with membranes of various sizes
- must be made of material, which is resistant to all chemicals to be used in the device

For the material of the device we chose polyoxymethylene (POM). We designed the device using CAD software SolidWorks 2012. All parts of the initial device where rectangular, but rectangular parts are easy to draw but difficult to produce.

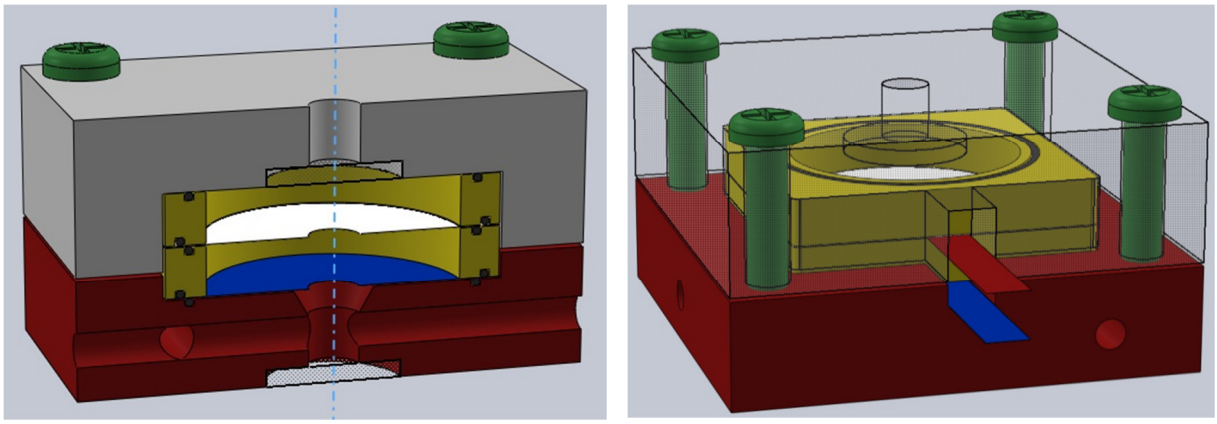

Figure 5. Initial device design

We realized that it's much easier to make the parts round in shape and producible on lathe.

To avoid large numbers of different parts we reduced the number of seals. We moved the seal to the side of the spacer ring that sealed the spacer directly against the body (Figure 6). To prevent sliding, the spacer rings were designed with edges and grooves (Figure 6). We decided to produce them with a 3D-printer, but realized that the edges are too small and could break off

easily. Therefore the edges were removed. The 3D-printed spacer rings were not leak-tight and to solve this issue, we covered the printed parts with silicone to make them leak-tight.

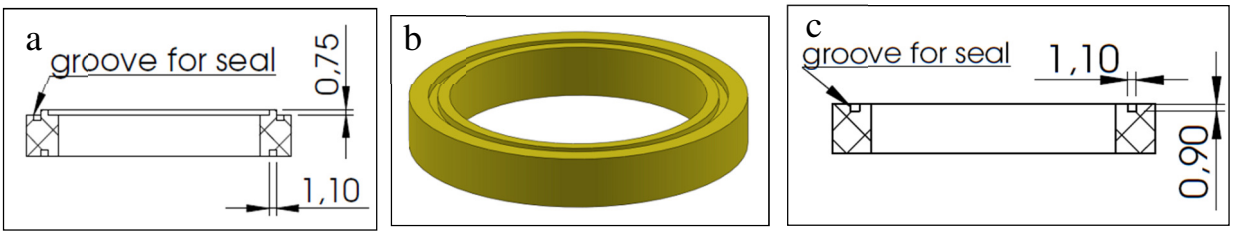

Figure 6. a: Spacer rings with edges; b: 3D model of the spacer ring; c: simple final spacer ring.

To make the device as universal as possible, the lower body part was designed with 2 pipe nozzles; the fluid flow is closed by 2 screws (Figure 7), which works as a valve and blocks the way to the chamber. The purposed of these nozzles is to avoid air bubbles in the two filled liquids and as well focused on an additional application of the device in the functionality of a pump.

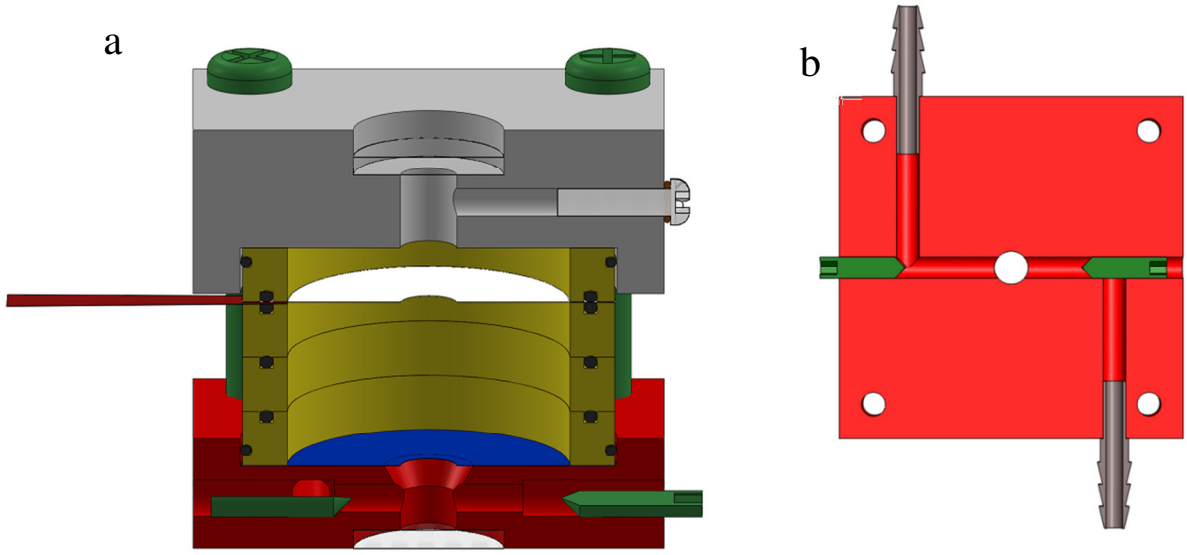

Figure 7. Experiment device, a: vertical cut view; b: horizontal cut view of the body.

The electrodes embedded in the experimental device were made of thin stainless steel sheets, with thickness of 30µm. To make experiments with membranes of various sizes, we made 2 special membrane supporting rings. These were made with small holes, in diameter of 20mm and another one in diameter of 10mm (Figure 8).

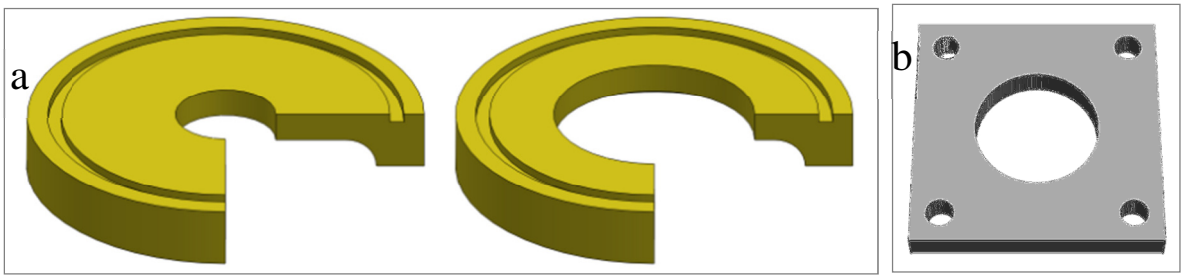

Figure 8. a: Cut view of support rings with hole diameter 10mm and 20mm; b: top plate

The first task was to apply the fluid lens device as an experimental set up to observe any membrane actuation displacement. Therefore we removed the upper part from the original device (Figure 7) and replace it with a top plate (Figure 8b). After filling the device with electrolyte and oil, it was meant to close with a removable glass plate, seen on Figure 9.

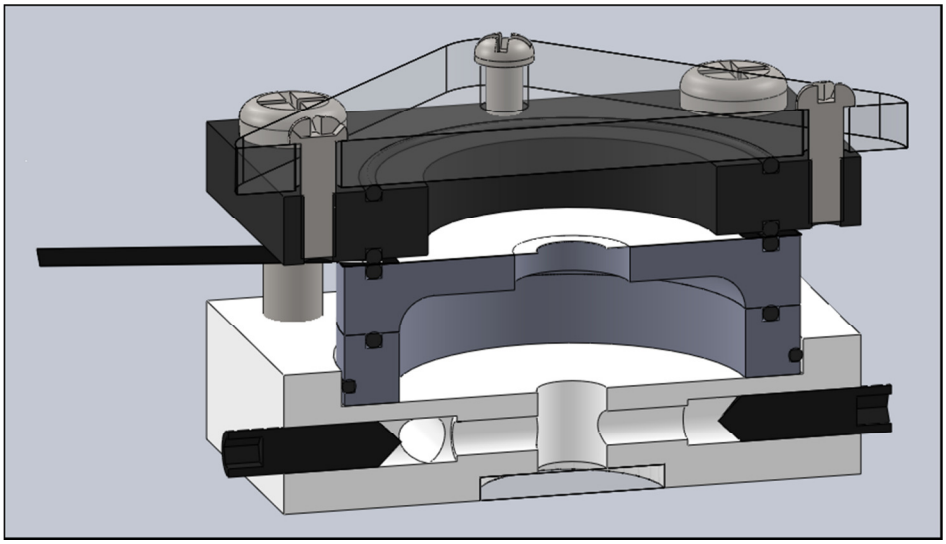

Figure 9. Final device before measurements, here with the 10mm support ring

3.1.2. Improving the device

When we started the measurements, we discovered that with tightening the screws we can very easily short-circuit the electrodes, because if the pressure is too high we compress the PVDF membrane that usually works as an insulator between the conductive polymer parts. To solve this problem one way was to tighten the screws very gently, the other way was to avoid screws by placing 2 big washers as pressure on the top plate (weight 25g each). Tightening gently caused additional problems: leakage appeared between the membrane and electrode contact (

Appendix 2). We replaced the plastic support rings with stainless steel rings, eliminated the leakage and obtained a better electrode contact to the membrane actuator. The fluid lens device in this design is able to measure the membrane actuator in bilayer functionality by placing the counterelectrode on the bottom of the working chamber (Figure 10). The counter electrode was 30µm thick and of the same size as the membrane actuator.

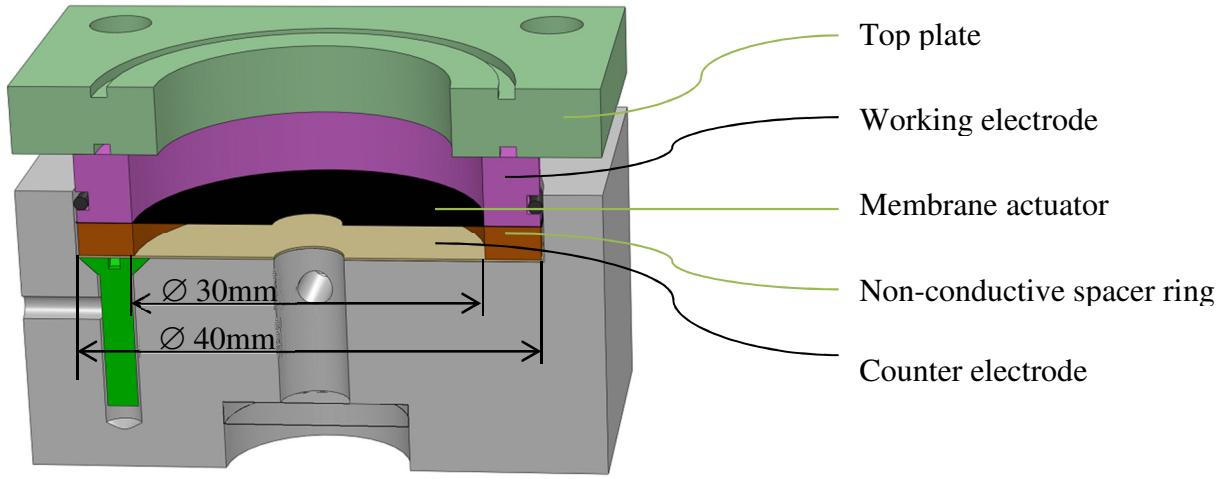

Figure 10. Setup for bilayer measurements dimensions

In the next step to make a more reliable contact to the counterelectrode and to the lower working electrode we created an electrical connection through the bottom of the device. We observed that the contact of the upper electrode needs adjustment to assure good electric contact. Therefore we placed an additional thin stainless steel sheet on it. To make sure that the upper electrode connection stainless steel sheet stays in place during the measurements we implemented a hole and a metal straw to hold it in place (Figure 12, blue straw). This construction is very easy to operate and showed good reliability in liquid lens experimental device functionality. The assembly instructions can be found in Appendix 2.

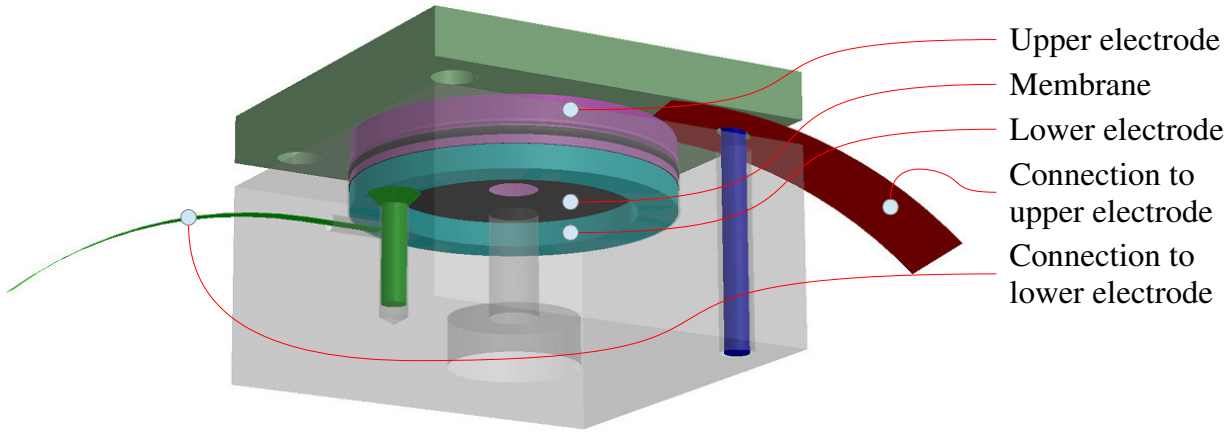

Figure 11. Final measurement device, the body is made transparent to illustrate the electrical connection points to the electrodes.

In real measurements we never used the spacer rings or the supporting rings. The spacer rings were designed to change the distance between bilayer actuator membranes and counter electrode, but we focused on measuring trilayer actuator membranes. Measuring various sizes of membranes was out of the scope for this work.

3.2. Measurements

The measurements were performed using a LabView program, specially made for measuring the movement properties of conductive polymers bilayer or trilayer. The LabView Program was controlling NI-2345 data acquisition system, both applying potential to the measurement device and recording the measurement results[19]. The displacement of the actuator membranes was recorded with an optical distance sensor (Keyence, LK-G10) simultaneously with the current output (enhanced by a current amplifier) under square wave potentials between ± 0.7V at different frequencies (0.00167-10Hz). The set up for the measurement instruments are shown at (Figure 12).

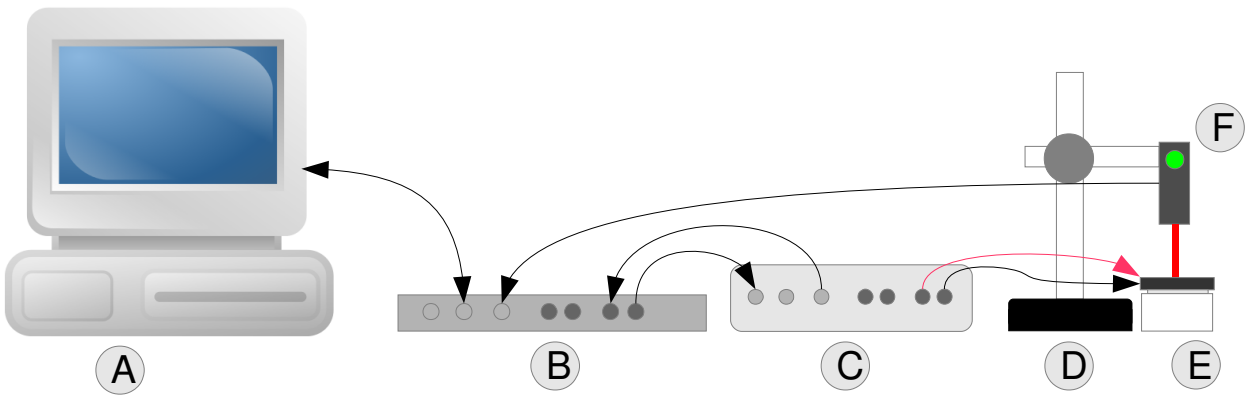

Figure 12. Schema of measurement instruments; A: computer, B: data acquisition system (SC-2345), C: power amplifier, D: stand for distance sensor, E: Fluid lens measurement device, F: distance sensor.

The image at Figure 13 shows the autofocus fluid lens device with membrane actuator included in operation mode.

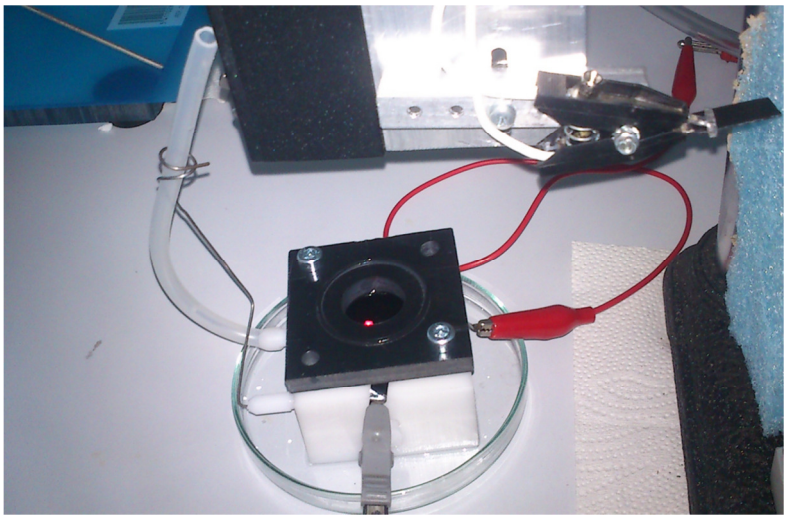

Figure 13. Autofocus fluid lens device with membrane actuator in operation mode

The device was filled with the electrolyte by using a pipette. The tube on the left (Figure 13) obtained the excess electrolyte to operate with a non-closed chamber below the membrane. When measuring the displacement of the membrane a small piece of black POM plastic was placed in the middle of the membrane actuator. The distance sensor measured the displacement of this piece, triggered by the membrane actuation. The red dot in the middle shows the laser beam reflection from the plastic piece.

4. RESULTS

4.1. PVDF membrane coated with conductive layer and deposited electrochemically with PPyTFSI (20µm each side)

4.1.1. PPyTFSI on gold plated PVDF (membrane A1)

The first actuator membrane was based on gold plated PVDF with electrochemically deposited PPy doped with LiTFSI in thickness of 20 µm on each side of the membrane (membrane A1). The electrolyte for actuation was selected 1.0M LiTFSI in propylene carbonate. The displacement results are listed in Table 3. The best membrane actuator displacement for this sample is shown on Figure 14.

Table 3: Membrane A1 displacements at square wave potentials (frequencies 0.1 - 0.00167 Hz)

frequency/Hz	displacement/µm	creep per cycle/µm
0.1	0.4	-
0.05	2,3	0.1
0.03333	4	0.8
0.01667	6.8	0.8
0.00833	7.2	0.15
0.00167	45	0.15

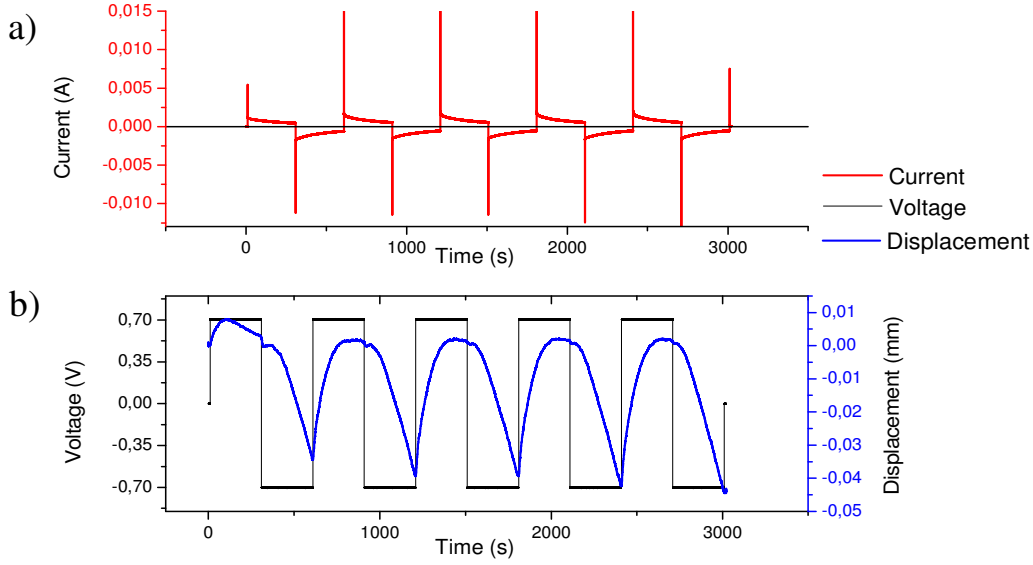

Figure 14. Membrane A1 in trilayer design in 1.0 M LiTFSI propylene carbonate at square wave potentials at applied voltage ± 0.7V (frequency 0.00167 Hz) of a) the current time curve and b) the displacement curve

The membrane actuation displacement (Figure 15b) shows at the first cycle irreversible displacement that we assumed relies on swelling effects in propylene carbonate. The second cycle shows reversible bending behaviour in the range of 45µm with little creep development after completing the numbers of cycles. If the starting and ending positions of the membrane actuator after cycling is different, creep occurs. Due to appeared short circuit of the membrane actuator A1 (Figure 14a) we applied a different set up of the membrane actuator in bilayer arrangement, one side of the membrane actuator was set as working electrode while on the other side a stainless steel ring was connected as a counter electrode. The device setup for bilayer measurement is shown in Figure 10. The results of the bilayer set up for the membrane A1 actuators are listed in the Table 4.

Table 4. The results of the membrane A1 as bilayer in 1.0 M LiTFSI electrolyte in propylene carbonate

frequency/Hz	displacement/µm	creep per cycle/µm
0.5	0.3	0
0.1	0.8	-0.03
0.033	1.3	-0.06
0.017	1.6	-0.3
0.0083	3	-0.4

The best actuator membrane displacement in bilayer functionality was found with 3 µm at 0.0083 Hz. This low displacement in comparison to the trilayer design of the PPyLiTFSI (Table 3) shows that the bilayer arrangement needs more adjustment to fulfill the requirements (chapter 1.3.1) for the autofocus fluid lens device.

In order to arrange the membrane actuator in its working design we cut a hole in the centre of the membrane by punch pliers with a diameter of 4mm, where in later arrangement the meniscus of the oil/electrolyte interface will appear (Figure 3). The results of the membrane A1 actuator displacement (with a hole in the centre) are listed in Table 5.

Table 5. Membrane A1 actuator (with a hole in the centre) in trilayer design resulting membrane displacements in 1.0 M LiTFSI propylene carbonate at square wave potentials (different frequencies) between ± 0.7 V.

frequency/Hz	displacement/µm	creep per cycle/µm	Comment
0.05	2.6	-	-
0.017	10	-	both types of ion movement present
0.0017	26	16.3	-

With a 4 mm hole in the centre of the membrane we observed smaller displacement at different frequencies (Table 5) but high creep development was observed as well.

For the working fluid lens measurement device we need to provide membrane actuators operating in aqueous electrolyte. To investigate which influence aqueous electrolyte has in membrane displacement we applied the same membrane in 1.0 M LiTFSI aqueous electrolyte (over night storage) in trilayer and bilayer arrangements. We observed no movement of the membrane A1 actuator that we assumed was caused by interaction of different solvents applied in this measurement. The results of this measurement are presented in Appendix 1. To avoid solvent exchange we applied for further measurements membrane actuators in trilayer functionality operating only in aqueous electrolyte.

4.1.2. PPyTFSI on chemical coated PVDF with PPy (membrane A2)

The difference between membranes A1 and A2 are the conductive coatings that appear for membrane A2 in chemical fixed PPy layer on PVDF (chapter 2.1). It was noticed that the membrane A2 actuator shows anion and cation effects at applied square wave potentials between ± 0.7V (Figure 17).

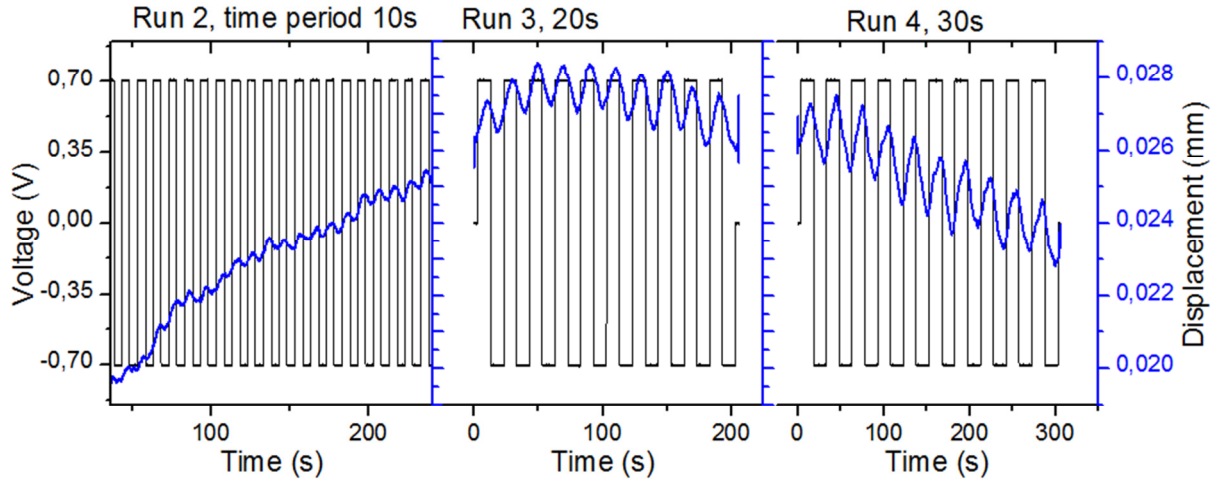

Figure 15. Measurement with membrane A2 in aqueous electrolyte (1.0M LiTFSI), at different applied frequencies (± 0.7V)

At frequency 0.1 Hz we observed for the first 4 cycles little displacements and after longer cycling time the displacement of the membrane A2 increased. This might be caused by certain training effect of conductive polymer actuators that expresses in forming after some time the right size of holes where the ion exchange takes place[22]. Lower frequency increased the

membrane actuator displacement. We observed that the membrane A2 actuator at frequency of 0.03 Hz shows an unexpected phenomena that during cycling from mainly anion driven actuation at the the first cycles changes to mainly cation driven actuation on the last cycle. The results are presented in Figure 17.

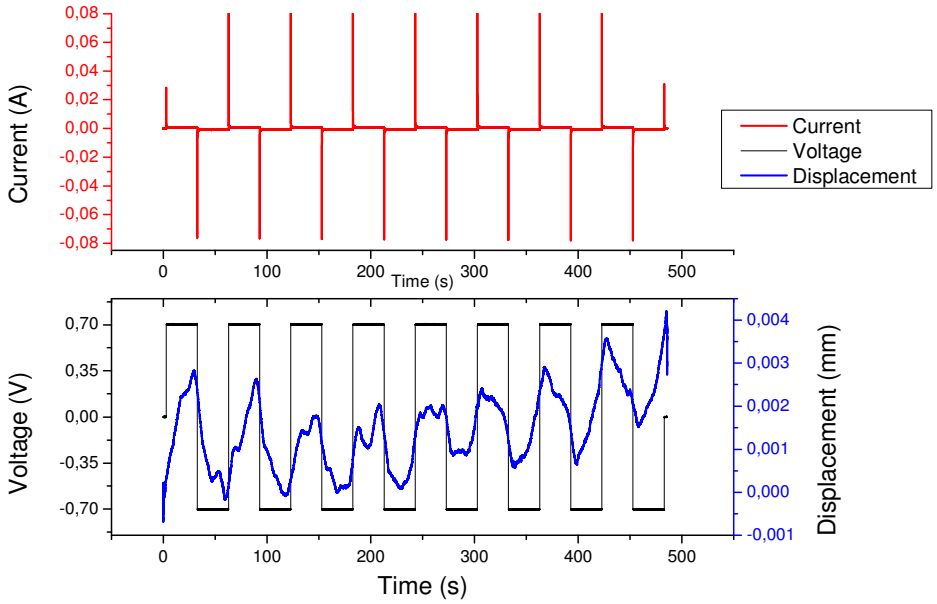

Figure 16. Mixed ion effects of membrane A2 in aqueous electrolyte (1.0M LiTFSI) at applied potential ± 0.7V at frequency 0.03Hz.

At applied potential 0.7V we could observe (Figure 16) anion motion in the PPy network that lead to the expansion and therefore the membrane actuator moved up. On the reduction at -0.7V the anions left from the PPy network and contraction appeared that induced the membrane actuator to move down. It was noticed that with further cycles a split of the displacement curve at 0.7V indicated that anions move in and cations move out (mixed ion process). During further cycling the membrane actuator displacement curve showed opposite directions. This means that some anions at reduction process don't leave the PPy network, providing a negative charge so that the cation motion in the polymer maintained the charge balance. To avoid anion and cation involvement in the actuation process we switched to a different conductive polymer based on PPy doped with DBS (chapter 2.1), where the big anion DBS^- immobilised partially in the PPy network[11] and therefore lead to mainly cation driven actuation at reduction (-0.7 V).

4.2. PVDF membrane coated chemically with PPy and deposited electrochemically with PPyDBS (20µm each side) (membrane B1)

Conductive polymer such as PPyDBS is well studied and their reversible volume change[15] at applied potential understood in mainly cation exchange during reduction[11]. The membrane B1 actuator displacement was caused by mainly cation driven actuation. With longer cycle number the membrane B1 actuator displacement showed improvements (Table 6).

Table 6. Actuator displacement of membrane B1 in 1.0M LiTFSI aqueous electrolyte at applied potential ± 0.7V (different frequencies)

frequencies/ Hz	displacement /µm	creep per cycle/µm	comment
0.1	0.3	0.2	
0.05	0.5	0	
0.033	0.5	-0.5	
0.01667	1.6	-0.6	
0.083	3.6	-0.9	
0.00167 (1)	17…40	-1.3	training effect
0.00167 (2)	44…62	-2.25	training effect

The maximum displacement with 62 µm was found at frequency of 0.00167 Hz and we could also observe the so called "training effect" (Table 6 in 0.00167 Hz (1) and (2)), described before at chapter 4.1.2 (Figure 15). The displacement of membrane B1 actuator is presented in Figure 17.

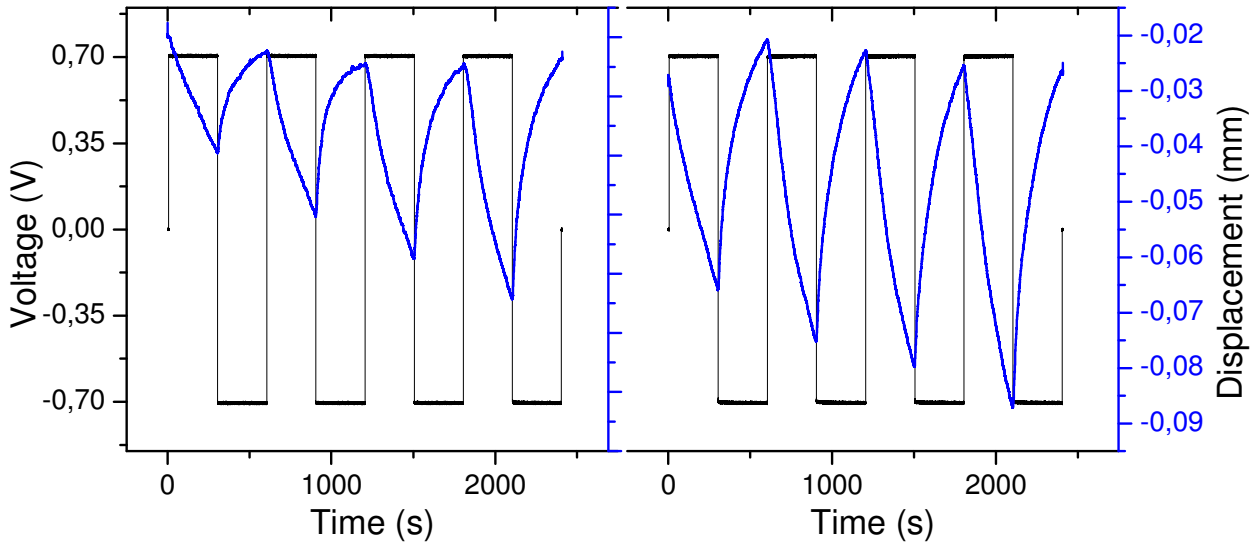

Figure 17. Membrane B1 actuator displacement at frequency 0.00167 Hz in 1.0 M LiTFSI aqueous electrolyte at applied potential ± 0.7 V.

With longer cycle time at 0.00167 Hz (Figure 17) we observed that the membrane B1 displacement increased. To further improve the membrane actuator displacement we decided to change to different thickness of the PPyDBS by applying shorter polymerization time. Additionally we changed the polymerization temperature to -5°C.

4.3. PVDF membrane coated chemically with PPy and deposited electrochemically with PPyDBS (2 µm each side) (membrane B2)

Earlier research[23] on PPyDBS bending trilayer showed that the thickness of the PPyDBS has an influence on displacement at different frequencies[24]. The membrane B2 actuator displacement results are presented in Table 10 and we obtained much higher displacements of the membrane B2 (371µm, 0.00167 Hz) compared to membrane B1 (62 µm, 0.00167 Hz). We observed that the creep of the membrane B2 was rear, which made this actuator membrane more suitable for the autofocus fluid lens application.

Table 7. Actuator displacement of membrane B2 in 1.0M LiTFSI aqueous electrolyte at applied potential ± 0.7V (different frequencies)

frequency/Hz	displacement/µm
1	0.3
0.5	3.5
0.1	16.2
0.05	22
0.03333	35
0.01667	69
0.00833	128
0.00167	371

The actuator membrane for the fluid lens measurements device (Figure 9) has a hole in the middle of the membrane (4mm in diameter) where the lens shape is formed. To investigate the influence of the membrane displacement by cutting a hole in the centre, we made measurements with and without the hole. The results are shown in Table 8.

Table 8. Actuator displacement of membrane B2 with and without a hole in 1.0M LiTFSI aqueous electrolyte at applied potential ± 0.7V (different frequencies)

modifications	run number	frequency/Hz	displacement /μm	Comment
no hole	1	0.0167	15.9	upper side dry
no hole	2	0.0167	24	both sides in electrolyte
no hole	3	0.0083	55.5	both sides in electrolyte
no hole	4	0.00167	293	both sides in electrolyte
no hole	5	0.0167	58.8	both sides in electrolyte
hole	6	0.0167	167	
hole	7	0.0083	300	
hole	8	0.00167	534	

We could observe that the membrane B2 actuator displacements nearly doubled if we cut a hole in the middle of the membrane (Table 8). We assume that the hole in the middle of the membrane affects a faster exchange of electrolyte during actuation and therefore higher displacement of the actuator membranes can be obtained.

4.4. Improvements

4.4.1. Simulation of membrane actuator in different cutting design

To improve the movement of a membrane actuator by cutting it in different shapes we applied different cutting designs (Figure 18). Recent studies on IPMC membrane actuators with cutting design (radial cuttings without internal ring) show improvement of the membrane displacement[25]. For our purpose we needed to keep a small ring in the middle to maintain the shape of the oil/electrolyte formed lens. The membranes were cut from outside to inside but 0.5 mm to the hole in the centre remained uncut (Figure 18). The pictures of templates used for cutting the membranes can be found in Appendix 3.

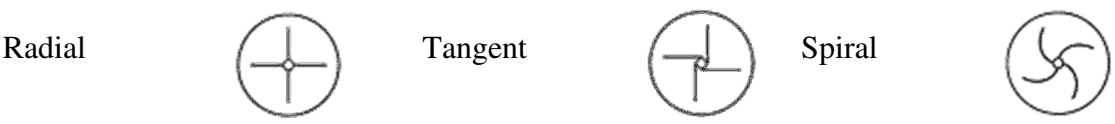

Figure 18. Different cutting design of the membrane actuator

We used SolidWorks simulation module (SimulationXpress) to study how different cutting designs are affecting the membrane actuator displacement. To simulate the membrane actuator we applied constant pressure on the surface as an actuation stimulus (Figure 19).

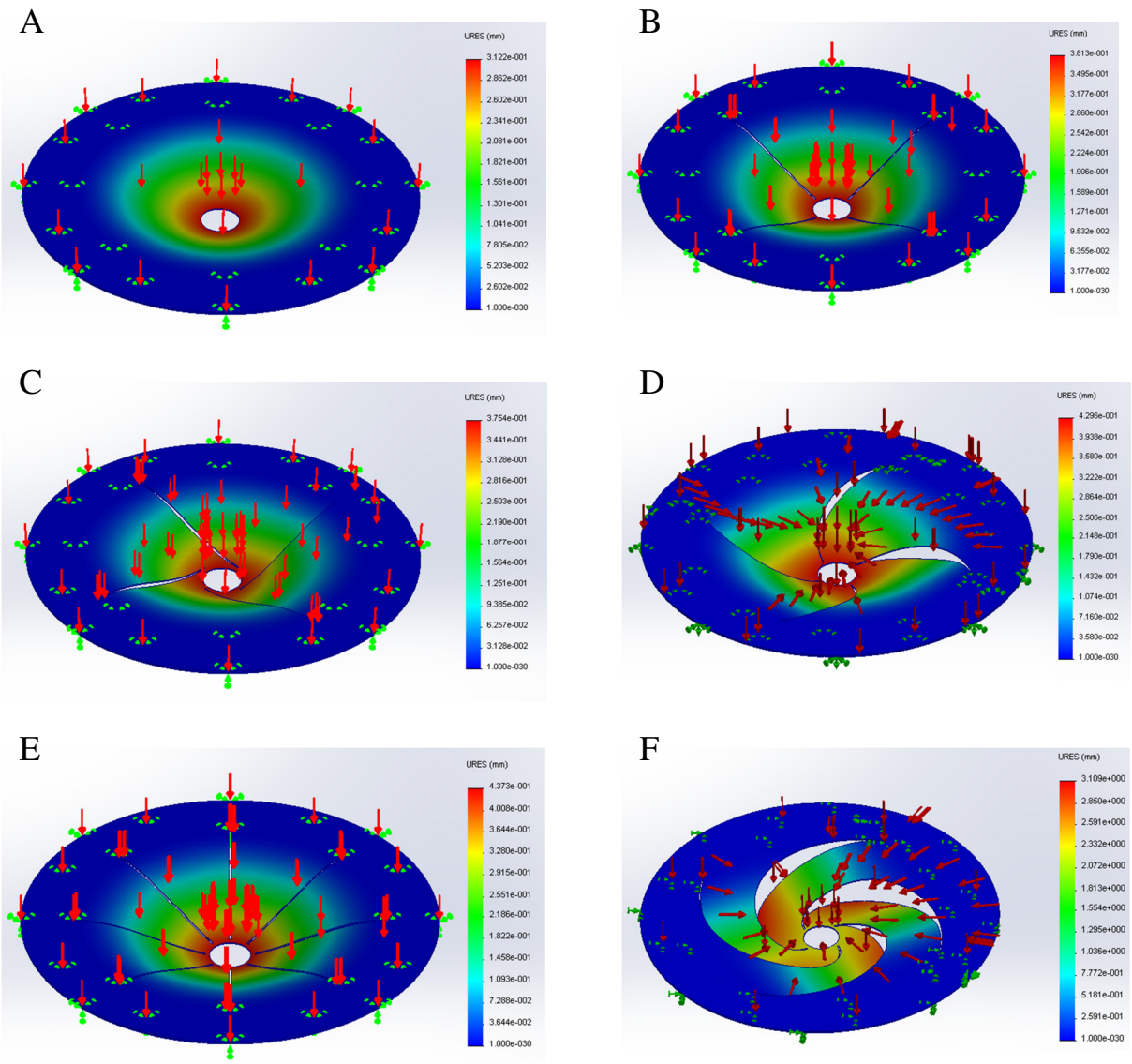

Figure 19. Simulations of different cutting designs of the membrane actuator in shape of A: without cutting, B: straight in 4 radial slices, C: tangent 4 slices, D: spiral (0.25 turn) 4 slices, E: tangent 8 slices and F: spiral ().75 turn) 4 slices

Figure 19 B-F shows shapes from the simulation and results that cutting in different shapes with maintaining an internal ring in the centre, has strong influence of the membrane actuator displacement. The theoretical results of the improvement in simulation are listed in Table 9.

Table 9. Membrane cutting design and actuator improvement from simulation

	Cutting design	Improvement theoretical
A	No cutting	
B	Radial 4 slices	22%
C	Tangent 4 slices	20%
D	Spiral 0.25 turn, 4 slices	38%
E	Radial 8 slices	40%
F	Spiral 0.75 turn, 4 slices	647%

We could observe that different cutting designs of the membrane B2 actuator show theoretically overall improvements of the membrane actuation. From simulation we found the highest improvement in the design in Figure 21-F. In contrast to the simulation the cutting design F showed no improvements in membrane actuation measurements.

By sliding the membrane in spiral cutting with 0.75 turn (Figure 21-F) we observed in the actuator displacement no uniform movement that derives from the asymmetric cutting form. The correlation between maximum displacements at different frequencies for different cutting designs of membrane B2 actuator are presented in Figure 21.

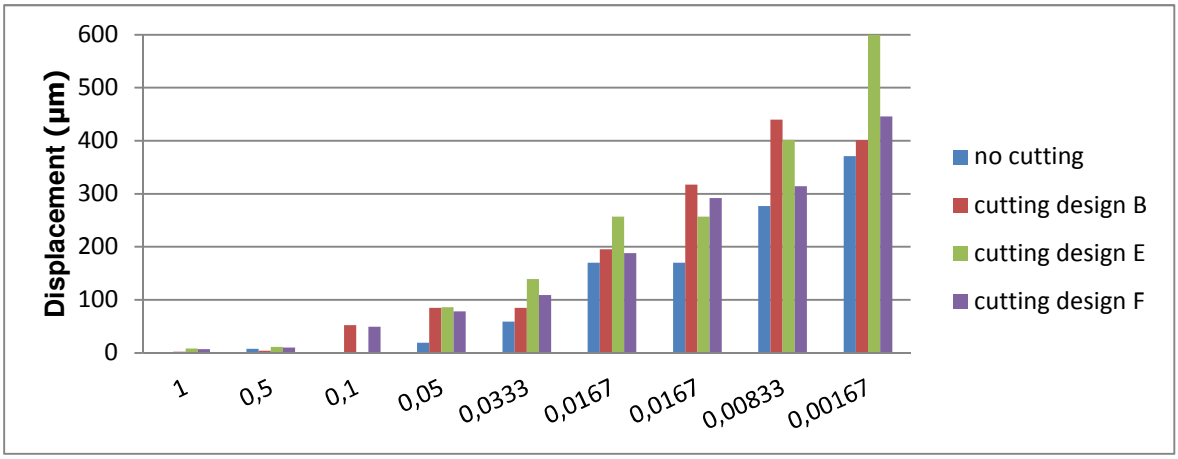

Figure 20. Comparison of membrane B2 actuator of no cutting (blue), cutting design B (red), cutting design E (green) and cutting design F (purple).

The best cutting design for membrane actuators movement in the measurements was found for the cutting design B (radial 4 slices) and E (radial 8 slices). The membrane B2 displacement for the cutting designs B and E is presented in Figure 21.

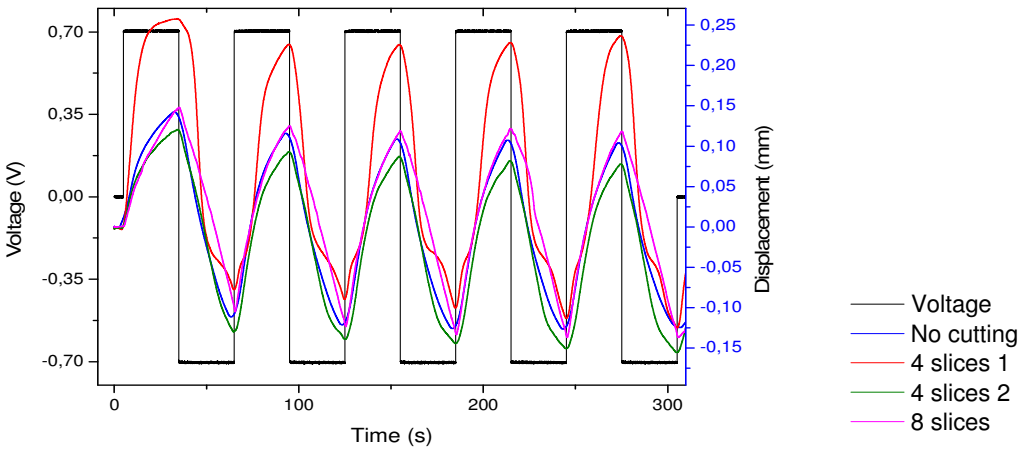

Figure 21. Membrane B2 actuation in 1.0 M LiTFSI aqueous electrolyte between ±0.7 V (frequency: 0.0167 Hz) without cutting and with cutting design B (radial 4 slices) and E (radial 8 slices)

We could observe in Figure 21 that the cutting design B (red curve) of the membrane B2 actuator shoed high displacement at the first 5 cycles and normed to a constant displacement at higher cycle numbers (green curve). The first high displacement of the fresh cut membrane B2 showed higher displacement. With higher number of cycles the displacement reduced as before and we obtained almost the same displacement size at continuing cycling with nearly no creep appearance. The displacement of nearly 200-300µm of the membrane B2 actuator in cutting design B and E showed that the required 200µm[4] for a lens shape can be achieved. To investigate the displacement with a given counter force we placed different weights on the membrane and investigated the displacement.

4.4.2. Counter force measurements

We measured the force of the membrane B2 in cutting design D by placing weights in the middle of the outer ring. To reduce the archimedes force (liquid push up force) the weights were placed on a thin wall plastic tube, which was long enough to reach above the electrolyte surface. The results of force measurements are given in Table 10.

Table 10. Results of the displacement with different weights

Membrane B2 cutting style D	frequency/Hz	weigth/mg	disp/mm
PPyDBS 2µm	0.0083	65	404
PPyDBS 2µm	0.0083	465	142.5
PPyDBS 2µm	0.0083	565	121

With increasing weight of 65–565mg we could observe a displacement decrease of the membrane B2 actuator as expected (Table 11). To investigate different frequencies of membrane B2 actuator without cutting the correlation between frequencies, displacement and force are given in Figure 22.

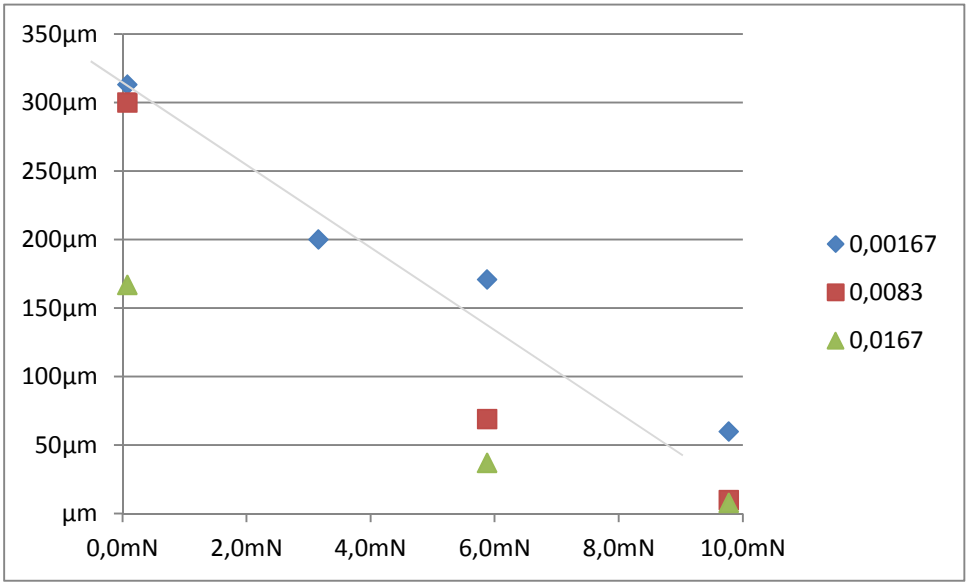

Figure 22. Membrane B2 displacement at different applied force

With high force of 9.8 mN we found at low frequency (0.00167 Hz) of the membrane B2 a displacement of 60 µm (Figure 23). Lower force of 0.1 mN increased the displacement in the range of 80%. There was a linear correlation between applied counterforce and achieved membrane displacement.

4.5. IPMC membrane C1 actuator

To obtain IPMC membrane actuators we activated the membranes by exposing them to boiling 1 M HCL solution (30 min) and stored them in aqueous 1 M $LiClO_4$ for 24 h, to assure that enough Li ions enter the Nafion membrane. The 4mm hole was made in the IPMC membrane C1 already

before the first measurement. The first measurement was made in pure water only to evaluate the displacement of the membrane. To investigate what influence electrolyte (1.0M LiTFSI) had on the displacement membrane C1, we stored the membrane over night in the electrolyte and operated it in our fluid lens measurement device in the same electrolyte. The results of the measurements of the membrane C1 at different frequencies are listed in Table 12.

Table 12. Results of the measurements with IPMC

	displacement/µm	
frequency/Hz	Electrolyte: H2O	Electrolyte: 1M LiTFSI in H2O
10	4.1	6.5
5	4.3	6.4
1	6	11.8
0.5	8.5	17
0.05	24	34.1
0.0333	35	34.3
0.01667	60	37
0.00833	37	37
0.00167	49.3	118

The membrane C1 displacement in pure water showed moderate displacement of 34 µm at 0.05 Hz but with lower frequency of 0.0083 Hz we could observe displacement of similar size in the range of 37 µm. This phenomenon was the result of the back relaxation at applied potential. By applying aqueous electrolyte instead of pure water we could observe higher displacement at certain frequencies with nearly double displacement. The typical displacement curves of the membrane C1 actuator is presented in Figure 23.

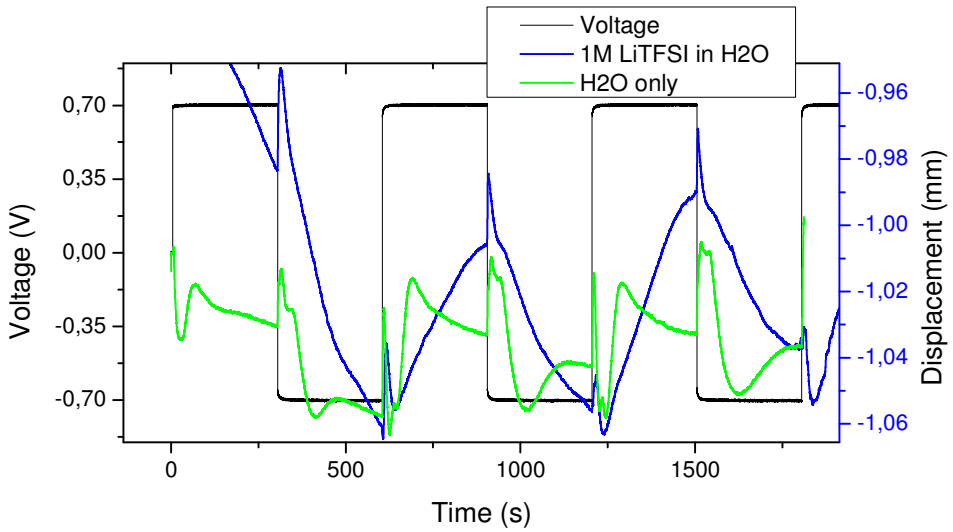

Figure 23. Membrane C1 displacement curves at applied potential between ± 0.7 V at frequency 0.00167 Hz in pure water (green) and 1M LiTFSI aqueous electrolyte (blue).

The membrane C1 displacement at applied frequency 0.00167 Hz showed in pure water (green, Figure 23) a fast back relaxation and low displacement. In comparison if the same membrane C1 was operated in 1M LiTFSI we could observe much higher displacement but also a more clear back relaxation. If the frequency is high enough, and the voltage polarity is switched before back relaxation takes place, then the membrane moves up and down similarly to conductive polymer membrane actuators. We could observe that the behavior of membrane C1 showed much simpler and more predictable (blue, Figure 23) displacement. Anyhow, the back relaxation limits these IPMC membrane actuators application in fluid lens device for focal length control.

4.6. Measurements with oil/electrolyte

In order to test the membrane actuator in its working conditions we applied silicon oil on the membrane B2 actuator but no meniscus between oil/electrolyte was formed. The reason for this effect can be found in wetting of the membrane by aqueous electrolyte. To avoid wettability of the aqueous electrolyte we applied a thin sheet of silicon grease on the membrane before filling the oil in the device. Unfortunately we observed certain contamination of the membrane actuator with silicon oil that terminates any displacement of the membrane actuator. To avoid this contamination with silicon oil we applied hydrophobic material based on PTFE grease (Addinol) in thin layer on the membrane actuator side facing the oil. Instead of silicon oil we used prolatium oil. We obtained no contamination and could observe a meniscus between oil/electrolyte formed over the cut hole in the centre of the membrane actuator. Nevertheless, the displacement of the membrane B2 actuator was not big enough (~20µm) to get the required $200\mu m^4$ change of the meniscus. Another uncertainty appeared as a huge creep during the membrane actuation that we assumed is due to the limited diffusion speed through the membrane at the upper side. To avoid further difficulties we improved the fluid lens measurement device.

5. NEW DESIGN OF AUTOFOCUS FLUID LENS DEVICE

The earlier fluid lens design (Figure 3) needed some improvements. To obtain lower displacement for changing the lens shape we needed the membrane actuator in trilayer design and certain conditions to be considered:

- both sides of membrane must be in the electrolyte
- oil or other compounds (grease) must not be in contact with the membrane

The new design and functionality of the fluid lens is presented in Figure 24.

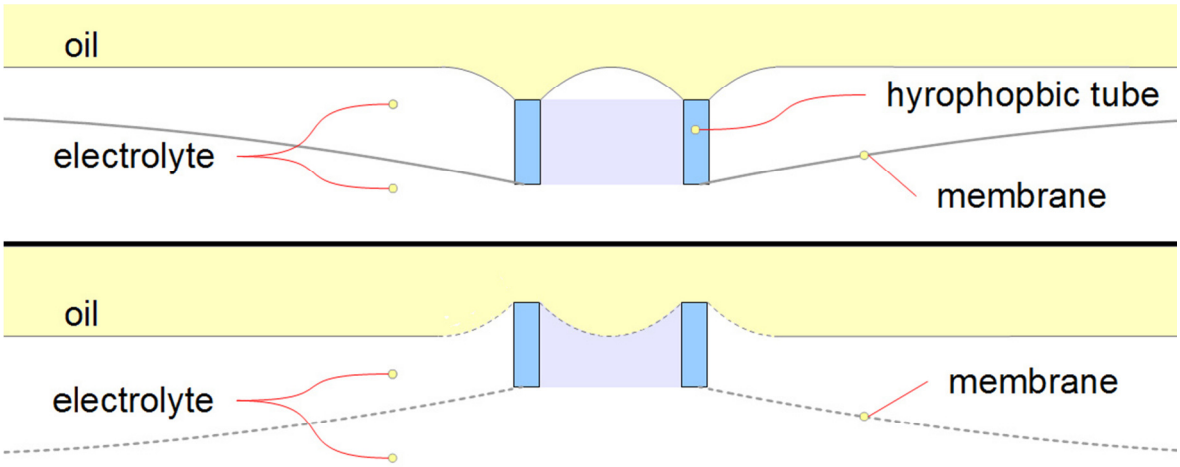

Figure 24. New design of the fluid lens with membrane actuator functionality in trilayer form

The new design of the fluid lens device (Figure 24) shows certain differences to the old design (Figure 3). The membrane actuator is immersed on both sides with electrolyte and the oil is placed on the electrolyte to avoid certain contamination of the membrane actuator. A new formed hollow tube made of POM (wall thickness 0.2mm), fixed with grease or glue on the membrane inner ring (beneath the hole) will form a meniscus between the oil/electrolyte interface.

When the membrane actuator moves down, the meniscus will create a positive lens and when the membrane actuator moves up, the meniscus will create a negative lens. To obtain changes of the meniscus a new measurement set up is presented in Figure 25.

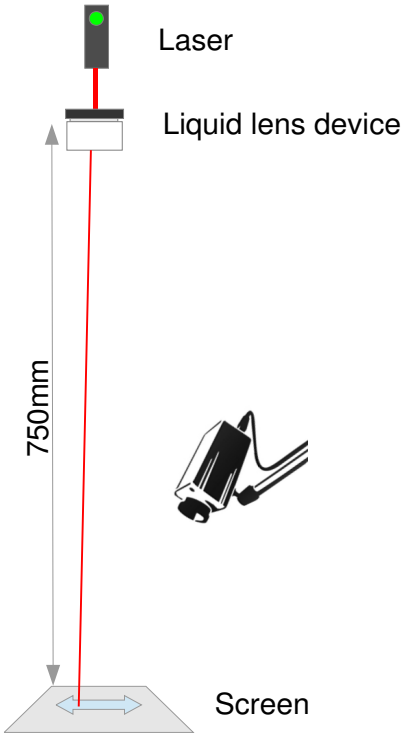

Figure 25. Setup for lens experiment

The laser beam is guided through the lens and by changing the lens focal length we alter the angle by which the laser beam is tilted from its original direction. During this experiment we achieved laser beam displacement (± 5mm) on the screen correlated to membrane B2 actuator displacement of 30µm at applied voltage (± 0.7V) at frequency of 0.00167Hz. The related images of the laser beam displacement are shown in Figure 26.

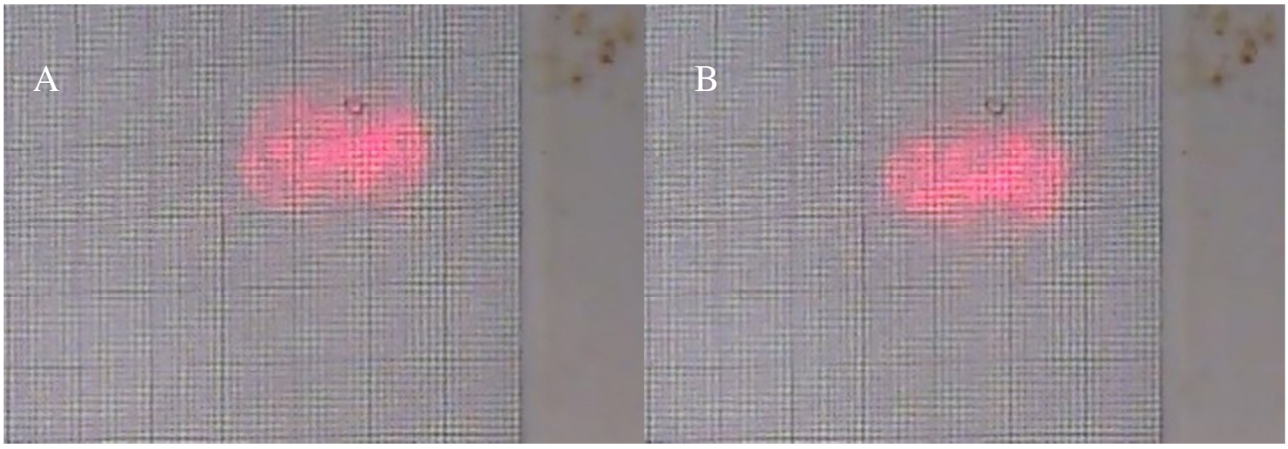

Figure 26 Images of laser beam displacement induced by membrane B2 actuator in auto focus fluid lens new design at applied potential (frequency 0.00167 Hz) of A: 0.7 V and B: -0.7 V

6. DISCUSSION

We built a new device that is applicable for electro active membrane actuators in trilayer functionality. We applied IPMC and CP membrane actuators in this work. Our main focus was set to conductive polymer membrane actuators due to the back relation issue that takes place for IPMC actuators[26]. To get a stable focal length change of fluid lens the displacement of the membrane actuators must be controllable. We applied two different types of conductive polymers based on PPyTFSI and PPyDBS.

In our first measurements with PPyTFSI, we observed that the membrane actuator showed only little displacement. The little displacement was induced by mixed ion effects that lead to further cycling to opposite displacement of the membrane at oxidation. We also saw that a huge creep appeared during several cycles. There can be several explanations to the creep: the electrolyte staying inside the polymer network after cycling [27] or conformational changes appear inside of the polymer network[28]. For the operation of a liquid lens, mixed ions, huge creep and direction changing displacement is not suitable. We applied another conductive polymer based on PPy doped with DBS anions. In changing the temperature from -33^{0}C to -5^{0}C and polymerization time (resulting PPy thickness: 2µm) at polymerization process in aqueous electrolyte we expected from previous research[26, 27] that we obtain mainly cation driven actuation. The DBS anion due to his organic nature and size stayed inside the PPy network after polymerization. That means that during the negative potential only one ion sort determines the actuation properties. Another parameter to get better control of the actuator displacement depends under which polymerization conditions the membrane actuator is formed. The results shown in chapter 3.3 (Table 10) indicate that the membrane B2 actuator (PPy 2µm) showed an improvement of displacement of 370µm at 0.00167 Hz (± 0.7V) compared to 60 µm (membrane B1, PPy 20µm) before. To understand why the thickness of the conductive polymer has an influence in more stable actuation is described in earlier research based on PPyDBS-PVDF-trilayer bending actuators[26]. We considered that the membrane B2 showed the best results in the displacement and good results by lifting counter force (~10mN). To improve the membrane actuation a new cutting design on membrane B2 actuator in radial, tangent or spiral cuttings (Figure 19-20) was applied to get a better displacement. Form a theoretical simulation to real measurements we could obtain an increase in membrane actuation in the range of 600µm at same applied potential and frequency with the cutting design B und E (Figure 21). The reason can be found on higher degree of freedom enabled by the cuttings. A strong controversy between the simulation and the

measurements was found in the spiral cutting design. This can be explained by obtaining different length of the cut stripes leading to different displacement properties[24] inducing minor membrane actuation.

First attempts with silicon oil on top of the membrane actuator showed new difficulties, that the attachment of the oil damaged the actuator due to spreading over the whole membrane and closing the pores of conductive polymer preventing the diffusion of ions.

To obtain membrane actuators in a trilayer functionality that both sides immersed into electrolyte we developed a new design of the arrangement of the membrane actuator. On the membrane actuator the inner ring is placed with a thin hollow tube and fixed on the membrane actuator (Figure 24). Electrolyte is filled on top of the membrane and oil filled on the electrolyte to the height of the tube (~ 2mm). At the tube a meniscus between oil and electrolyte was formed and by changing the membrane B2 actuator in trilayer functionality, we obtained reversible displacement in the range of 30µm with lens changing properties (Figure 25). The reason of the 200µm[4] estimated membrane displacement before was the originally simulated membrane bilayer functionality. From our research on the membrane actuators in bilayer arrangement we could obtain very little displacement but with membrane actuator in trilayer functionality with cutting design the displacement could be enhanced in the range of 500%.

With this new knowledge we are able to develop a fluid lens with variable focal length based on conductive polymer membrane actuators. The membrane actuation speed, the durability and membrane dimension need further improvements.

7. CONCLUSION

In this work we constructed a device for fluid lens operation. The lens change of the formed meniscus between oil/electrolyte is influenced by membrane actuator displacement based on electroactive polymers, where in the middle of the membrane a hole is formed. We investigated ionic polymer metal composite and conductive polymer in membrane actuators arrangement. Due to the back relaxation appearing in IPMC membrane actuator we concentrated on the performance of conductive polymers, influenced by different electrolyte, solvent and polymerization conditions. PPy doped with DBS in thickness of 2µm placed on each side of the before conductive coated PVDF membrane showed the best displacement and force (10 mN) in the range of 60µm at applied potential ± 0.7V (frequency 0.00167Hz). To improve the displacement of the membrane actuator by different cutting designs nearly doubled the displacement. The original principle of the liquid lens proved to be inoperative. To obtain focal length changes in liquid lens, a new design of the liquid lens was developed and we could detect focal length change in correlation to the applied potential that lead to membrane displacement. With this new design it is for the first time possible to build low power liquid lens.

I would like to thank my supervisor Prof. Rudolf Kiefer for his professional advice and guidance. I also express my gratitude to Rauno Temmer for his technical assistance and support, as well as my whole family and friends for their patience and understanding.

LITERATURE

1. http://www.varioptic.com/technology/liquid-lens-autofocus-af/ (cited 23.03.2013)
2. B. Berge, J. Peseux,“Variable focal lens controlled by an external voltage: an application of electrowetting”, Eur.Phys. J., 159-163, 2000
3. D., Graham-Rowe, Liquid lenses make a splash, Nature photonics, 2-4, 2006
4. R. Kiefer, R. LuoH, Autofocus fluid lens device for EAP membranes, Intern Report, Industrial Technology Research Technology, 2010
5. R.H. Baughman, Conducting polymer artificial muscles, Synth. Met.78, 339–353, 1996
6. A. Kraft, A.C. Grimsdale, A.B. Holmes, Electroluminescent conjugated polymers-seeing polymers in a new light Angew. Chem. Int. Ed. 37, 402–428, 1998
7. J.G. Killian, B.M. Coffey, F. Gao, T.O. Pochler, P.C. Searson, Polypyrole composite electrodes in an all-polymer battery system, J. Electrochem. Soc.143, 936, 1996
8. N. Leventis, Polymers in electrochromics, Polym. News 20, 5-18, 1995
9. J.N. Barisci, C. Conn, G.G. Wallace, Conducting polymer sensors, Trends Polym. Sci. 4, 307–311, 1996
10. E. Smela, Conjugated polymer actuators for biomedical applications, Adv. Mater., 15, 481, 2003
11. J. Heinze, B. A. Frontana-Uribe, S. Ludwigs, "Electrochemistry of Conducting Polymers—Persistent Models and New Concepts", Chem. Rev., 110(8), 4724-4771, 2010
12. S. Maw, E. Smela, K. Yoshida, R.B. Stein, Effects of monomer and electrolyte concentrations on actuation of PPy(DBS) bilayers, Synth. Met., 155, 18, 2005
13. S. Maw , E. Smela, K. Yoshida, P. Sommer-Larsen, R. B. Stein, The effects of varying deposition current density on bending behaviour in PPy(DBS)-actuated bending beams, Sensor Actuat. A-Phys., 89, 175-184, 2001
14. S. Shimoda, E. Smela, The effect of pH on polymerization and volume change in PPy(DBS), Electrochim. Acta 44, 219-238, 1998
15. R. Kiefer, D. G. Weis, J. Travas-Sejdic, G. Urban, J. Heinze, "Effect of electrochemical synthesis conditions on deflection of PEDOT bilayers", Sens. Actuators, B, 123, 379-383, 2007

16. R. Kiefer, G.A. Bowmaker,P.A. Kilmartin, J. Travas-Sejdic, Effect of polymerization potential on the actuation of free standing poly-3,4-ethylenedioxythiophene films in a propylene carbonate electrolyte, Electrochim. Acta, 55, (3), 681-688, 2010

17. R. Kiefer, D. G. Weis, A. Aabloo, G. Urban, J. Heinze, Dependence of polypyrrole bilayer deflection upon polymerization potential, Synth. Met.172, 37-43, 2013

18. R. Temmer, I. Must, F. Kaasik, A. Aabloo, T. Tamm, Combined chemical and electrochemical synthesis methods for metal-free polypyrrole actuators, Sensors Actuat. B-Chem., 166-167, 411–418, 2012

19. Shahinpoor M and Kim K J, Ionic polymer–metal composites: I. Fundamentals Smart Mater. Struct. 10, 819–33, 2001

20. V. De Luca, P. Digiamberardino, G. Di Pasquale, S. Graziani, A. Pollicino, E. Umana, M. G. Xibilia, Ionic Electroactive Polymer Metal Composites: Fabricating, Modeling, and Applications of Postsilicon Smart Devices, J Polym. Sci. Pol. Phys., 51, 699–734, 2013

21. S. Tadokoro, S. Yamagami, T. Takamori, K. Oguro, In Proceedings of SPIEs Smart Materials and Structures EAPAD: March, New Port Beach, CA; SPIE, Bellingham, WA, 92–102, 2000

22. T. F. Otero, H.-J. Grande, J. Rodriguez, J. Phys. Chem. B 101, 3688, 1997

23. R. Kiefer, X. Mandviwalla, R. Archer, S.S. Tjahyono, H. Wang, B. MacDonald, G.A. Bowmaker, P.A. Kilmartin, J. Travas-Sejdic, The application of polypyrrole trilayer actuators in microfluidics and robotics, in: Electroactive Polymer Actuators and Devices (Eapad), E9271, 2008

24. R. Kiefer, R. Temmer, T. Tamm, J. Travas-Sejdic, P. A. Kilmartin, A. Aabloo, Conducting polymer actuators formed on MWCNT and PEDOT-PSS conductive coatings, Synth, Met. 171, 69-75, 2013

25. S. Sareh, J. Rossiter, Kirigami artificial muscles with complex biologically inspired morphologies, Smart Mater. Struct., 22 , 014004 (13pp), 2013

26. E Shoji, D Hirayama, Effects of humidity on the performance of ionic polymer-metal composite actuators: experimental study of the back-relaxation of actuators, J. Phys. Chem. B, 111, 11915–11920, 2007

27. K. Tominaga, K. Hamai, B. Gupta, Y. Kudoh, W. Takashima, R. Prakash, I. Kaneto, Suppression of electrochemical creep by cross-link in polypyrrole soft actuators, Physics Procedia, 14, 143–146, 2011

28. J. D. Madden, D. Rinderknecht, P. A. Anquetil, I. W. Hunter, Creep and cycle life in polypyrrole actuators, Sensors and Actuators A, 133, 210–217, 2007

ELEKTROAKTIIVSETEL POLÜMEERIDEL PÕHINEVA MUUDETAVA FOOKUSKAUGUSEGA VEDELIKLÄÄTSE SEADME KONSTRUEERIMINE JA AKTUAATORI SUUTLIKKUSE UURIMINE

Harti Kiveste

KOKKUVÕTE

Muudetava kujuga vedelikläätse on seade milles läätse moodustab vedeliku tilk või kahe erineva vedeliku abil moodustatud menisk. Nagu näiteks Variopticsi välja töötatud vedelikläätse, milles läätse moodustab vee ja õli ühenduskohas tekitatud hemisfääriline menisk, kus kõrgepinget rakendades saab meniski kõverusraadiust ja seega läätse fookuskaugust muuta.

Käesoleva töö eesmärk oli projekteerida ja ehitada elektroaktiivsetel polümeeridel põhinevate membraanliikurite (*membrane actuator*) uurimist võimaldav seade, mis samas oleks kasutatav ka muudetava kujuga vedelikläätse konstrueerimiseks, kus läätse moodustab membraani keskele tehtud ümmarguses avas kokku puutuvate õli ja vee tekitatud menisk ning membraanliikuri liigutamine muudab meniski kõverusraadiust/läätse fookuskaugust. Teine eesmärk oli kasutades tehtud seadet viia läbi mõõtmiskatsed vedelikläätse fookuskauguse muutmiseks sobiva membraanliikuri leidmiseks.

Uuriti erinevaid elektroaktiivsetel polümeeridel baseeruvaid membraanliikureid, IPMC, polüpürrool dopeeritud TFSIga ja polüpürrool dopeeritud DBSiga, mis olid polümeriseeritud erinevatel tingimustel (temperatuur, kestus, kasutatud lahusti). Aktuaatori liigutusulatust uuriti erinevates elektrolüütides või erinevaid koormusi rakendades erinevatel sagedustel (10Hz – 0,00167Hz) rakendades neile ristkülikpinge vahemikus +0,7V…-0,7V. Uuritavate membraanliikurite läbimõõt oli kõikidel juhtudel 30mm. Liikumisulatuse suurendamiseks tehti membraanidesse erineva kujuga lõikeid. Kõige suuremaid nihkeid membraani keskele tehtud ava juures näitas membraanliikur, kus PPyDBS oli 2µm kihina polümeriseeritud 110µm paksuse PVDF membraani kummalegi küljele ning millesse oli tehtud radiaalselt 8 lõiget. Maksimaalseks nihkeks mõõdeti 785µm.

Katsetused esialgase läätse konfiguratsiooniga ei olnud edukad. Membraani nihe oli oodatust palju väiksem. Kui membraa999ni liikumisulatuse mõõtmiseks tehtud eksperimentides oli liikur täielikult elektrolüüdi sees, siis läätse konfiguratsioonis oli elektrolüüdiga kokkupuutes ainult membraani üks külg. Eelnevalt tehtud mõõtmised andsid kinnitust, et kui muuta vedelikläätse

konfiguratsiooni selliselt, et membraanliikur oleks mõlemalt poolt elektrolüüdi sees ning õli või mõne teise ainega kokkupuude oleks samuti võimalikult väike, siis on võimalik meniski kuju/vedelikläätse fookuskaugust muuta. Vedelikläätse uue konfiguratsiooni testimiseks läbiviidud eksperiment osutus edukaks. Läätse fookuskaugus muutus nii, et läätse läbinud laserkiire tekitatud valguslaik liikus ekraanil ±5mm, vastavalt membraanliikurile rakendatud pinge polaarsusele.

Appendix 1

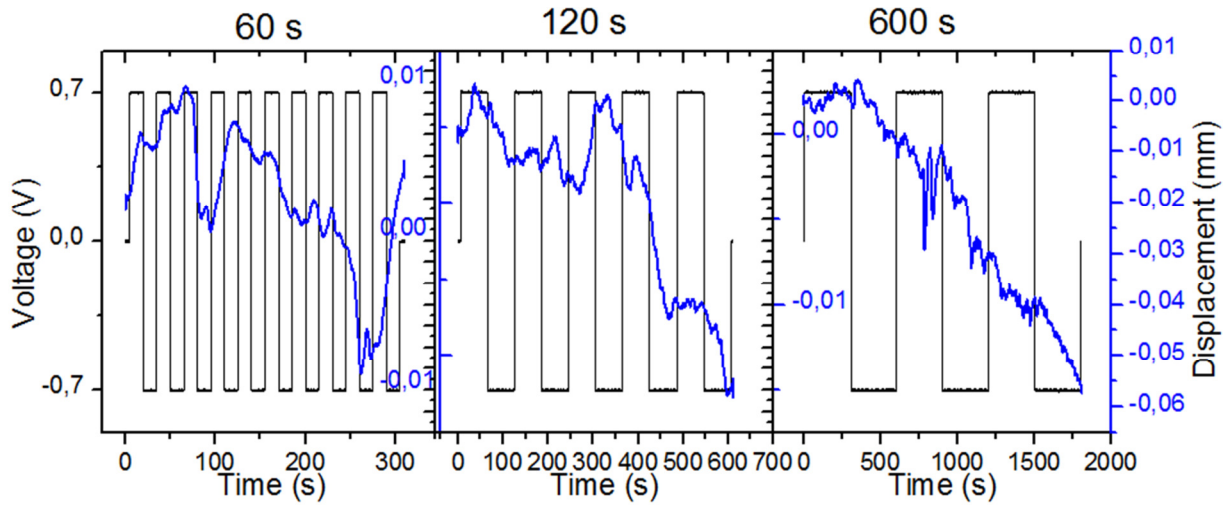

The results of membrane A1 in aqueous electrolyte measured as trilayer

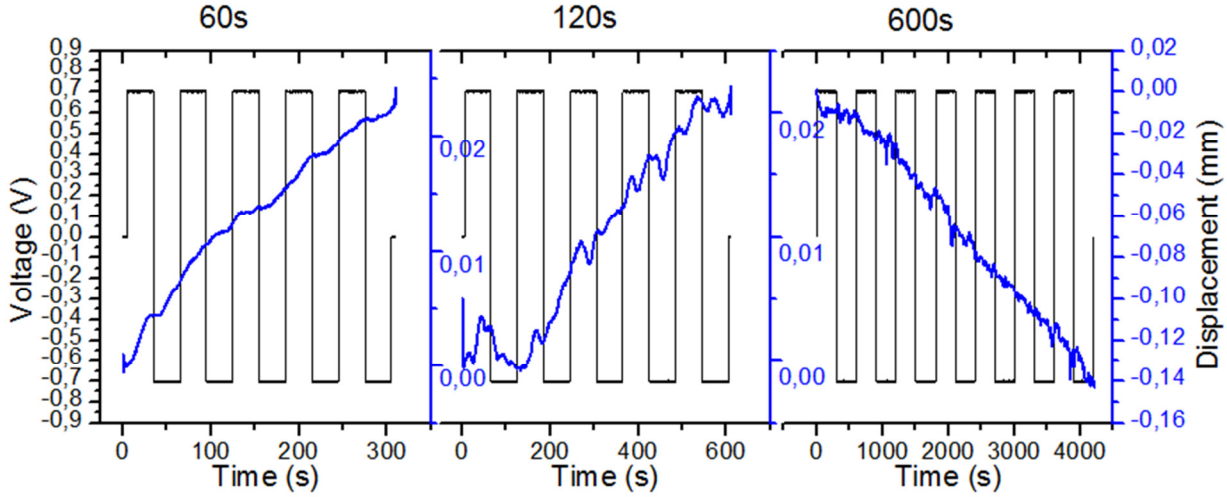

The results of membrane 1 in aqueous electrolyte measured as bilayer

Appendix 2. Device assembly instructions

a) trilayer configuration

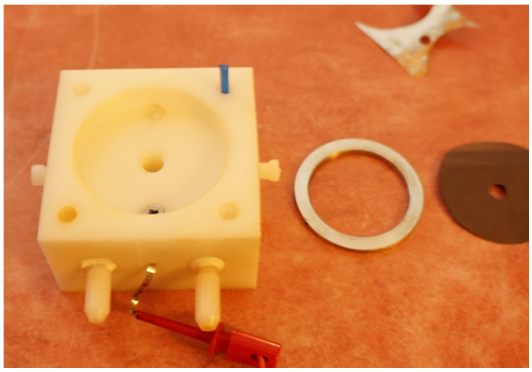
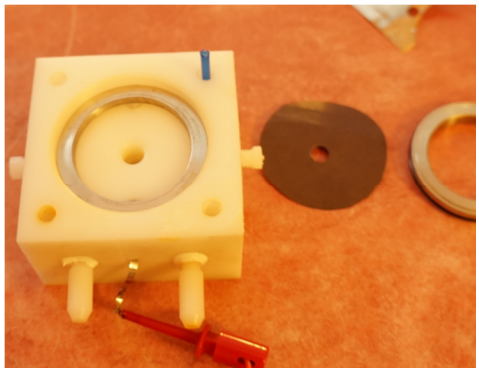
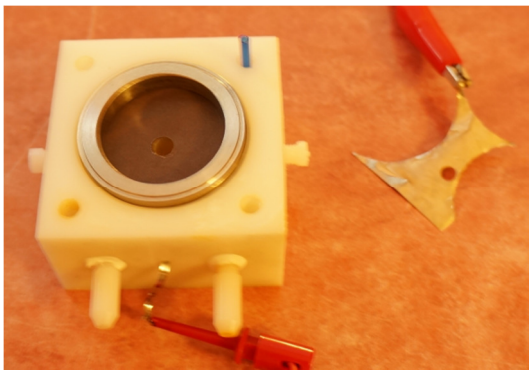
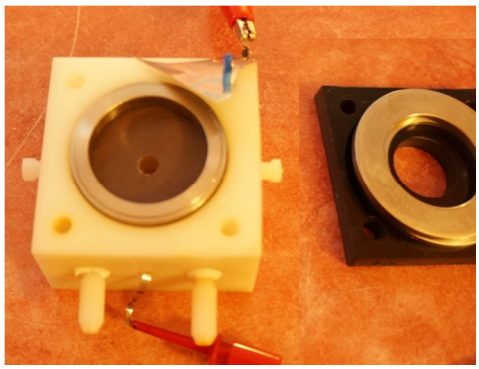
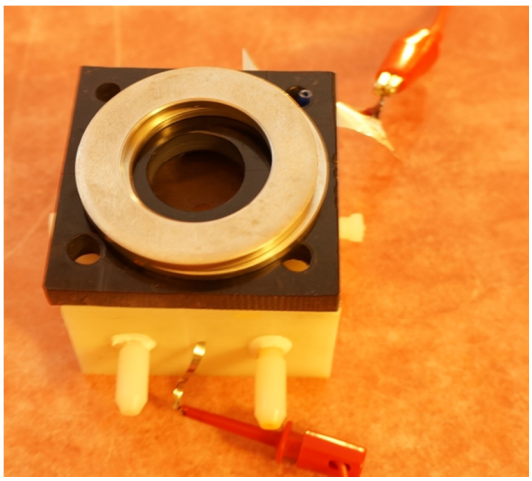
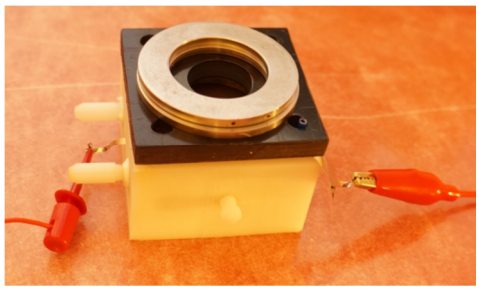

b) bi-layer configuration

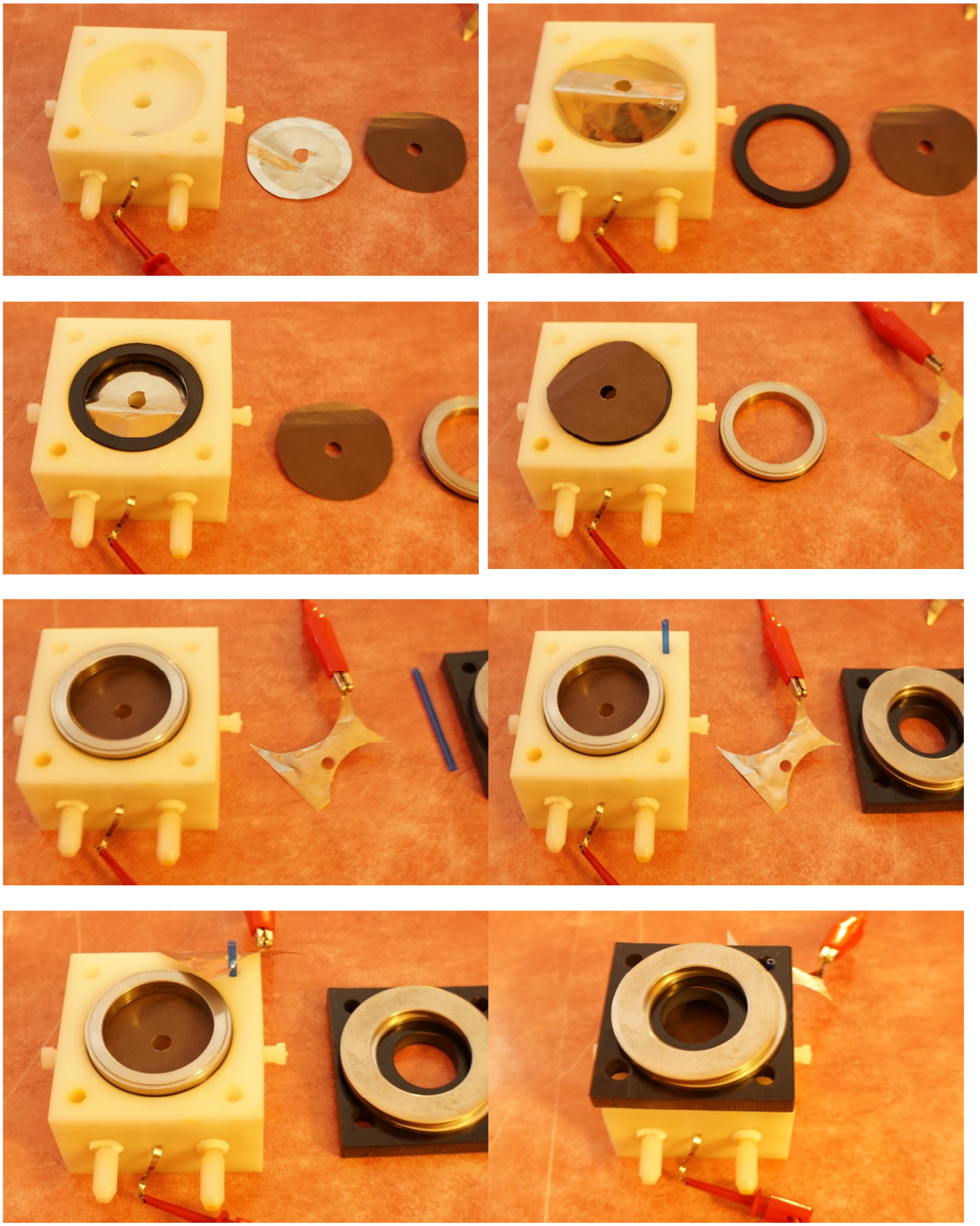

c) trilayer configuartion (initial version of the device)

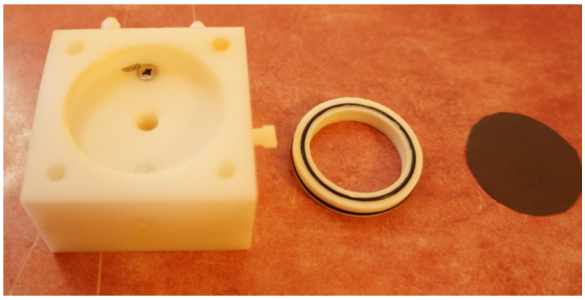
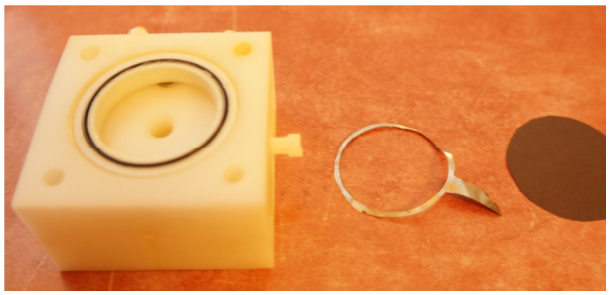
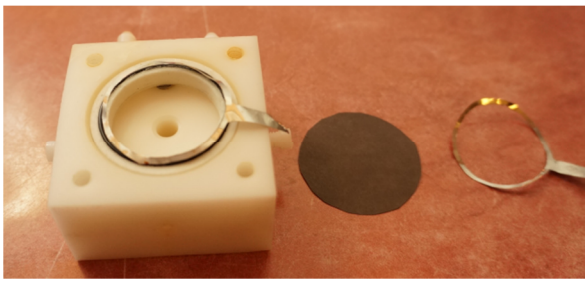
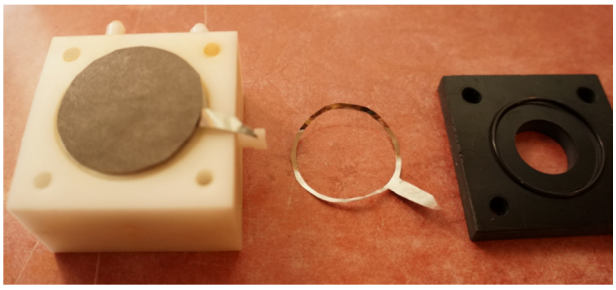
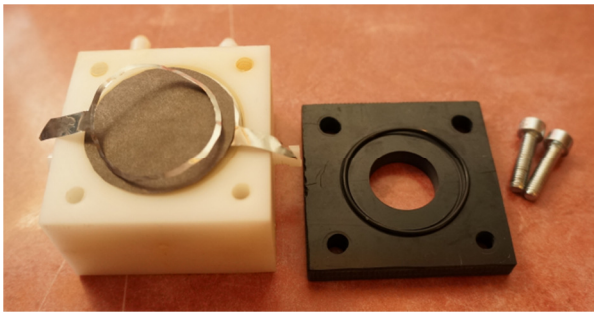
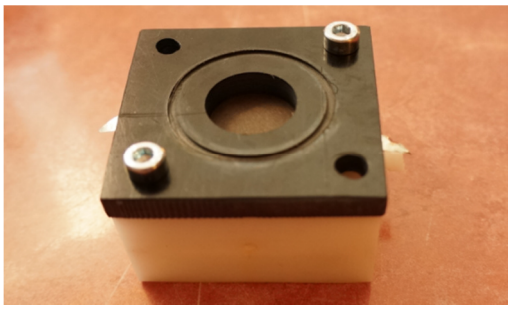
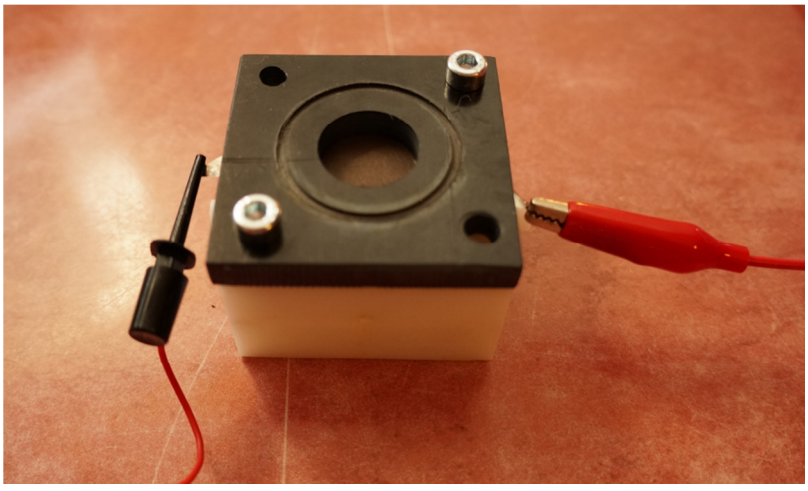

Appendix 3. Cutting templates

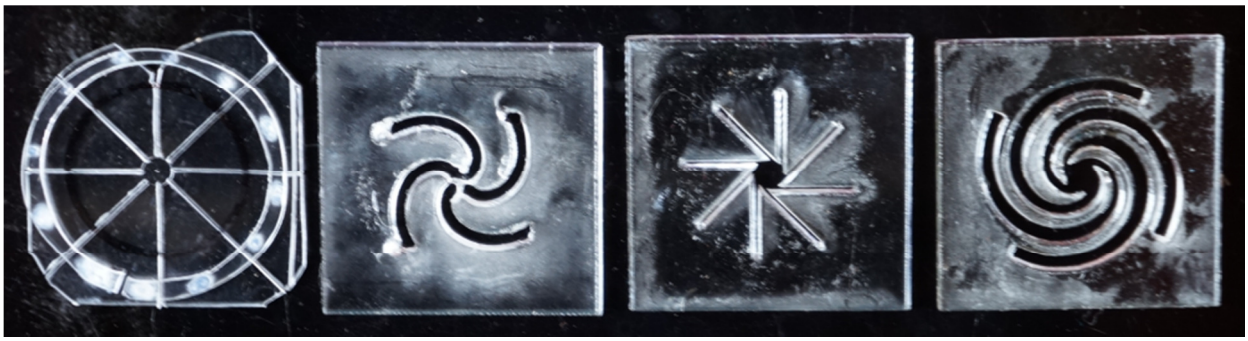

Appendix 4. Polymerization curves of membrane B1

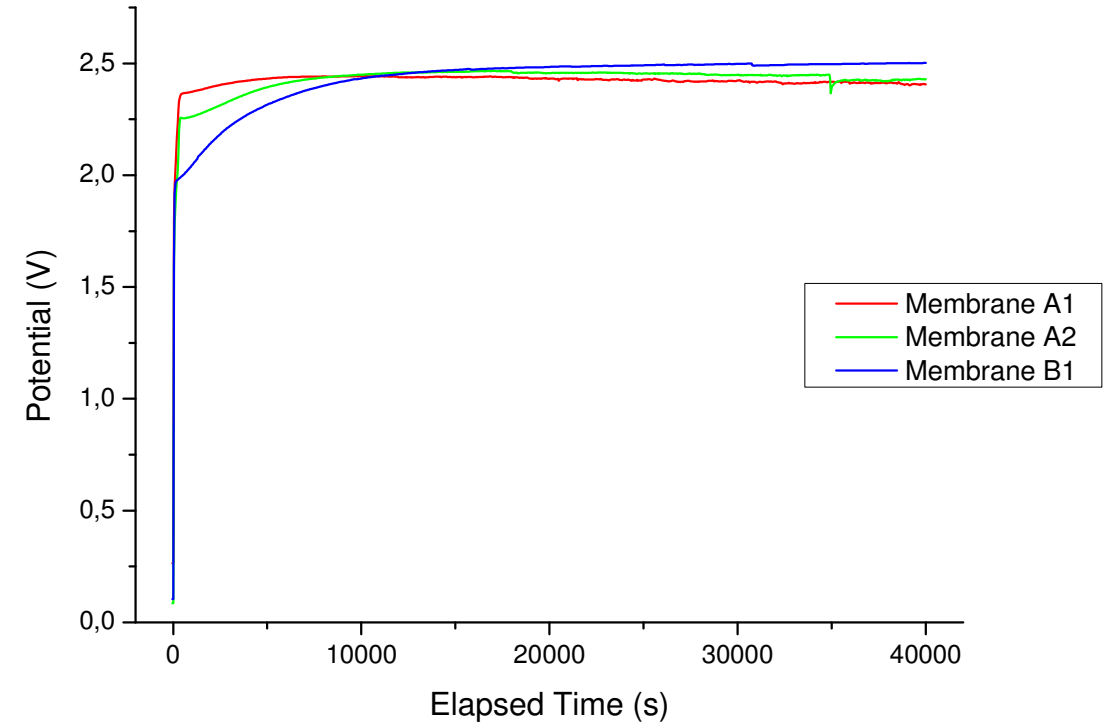

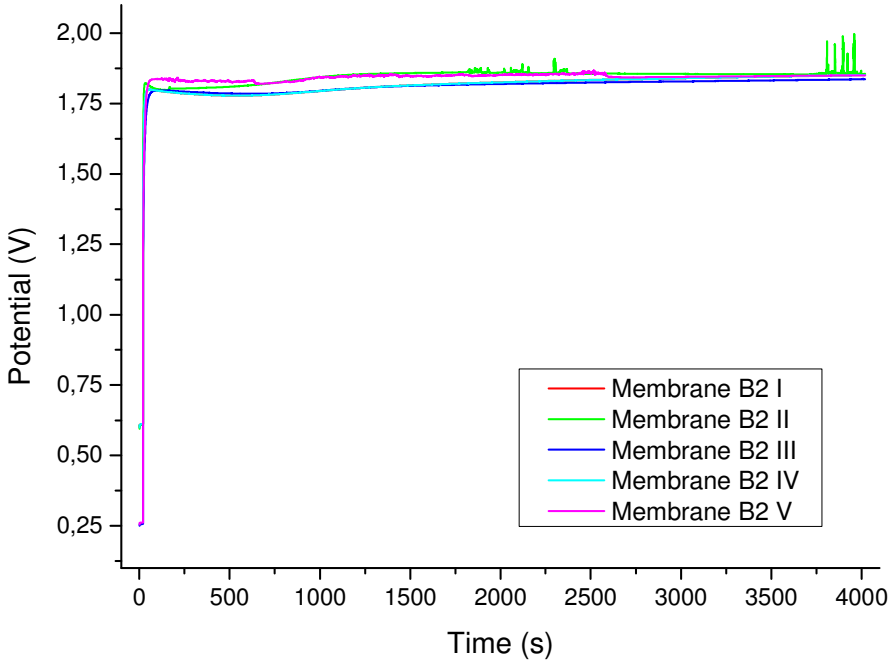

Lihtlitsents lõputöö reprodutseerimiseks ja lõputöö üldsusele kättesaadavaks tegemiseks

Mina, Harti Kiveste
(sünnikuupäev: 6.02.1981)

1. annan Tartu Ülikoolile tasuta loa (lihtlitsentsi) enda loodud teose
FLUID LENS DEVICE CONSTRUCTION AND ACTUATOR PERFORMANCE BASED ON ELECTRO ACTIVE POLYMERS,

mille juhendaja on professor Rudolf Kifer

1.1. reprodutseerimiseks säilitamise ja üldsusele kättesaadavaks tegemise eesmärgil, sealhulgas digitaalarhiivi DSpace-is lisamise eesmärgil kuni autoriõiguse kehtivuse tähtaja lõppemiseni;
1.2. üldsusele kättesaadavaks tegemiseks Tartu Ülikooli veebikeskkonna kaudu, sealhulgas digitaalarhiivi DSpace´i kaudu kuni autoriõiguse kehtivuse tähtaja lõppemiseni.

2. olen teadlik, et punktis 1 nimetatud õigused jäävad alles ka autorile.

3. kinnitan, et lihtlitsentsi andmisega ei rikuta teiste isikute intellektuaalomandi ega isikuandmete kaitse seadusest tulenevaid õigusi.

Tartus, **23.05.2013**